Eur. Phys. J. C (2012) 72:1839
DOI 10.1140/epjc/s10052-011-1839-3

THE EUROPEAN PHYSICAL JOURNAL C

Regular Article - Experimental Physics

Forward energy flow, central charged-particle multiplicities, and pseudorapidity gaps in W and Z boson events from pp collisions at $\sqrt{s} = 7$ TeV

The CMS Collaboration*
CERN, Geneva, Switzerland

Received: 2 October 2011 / Revised: 2 November 2011 / Published online: 20 January 2012

Abstract A study of forward energy flow and central charged-particle multiplicity in events with W and Z bosons decaying into leptons is presented. The analysis uses a sample of 7 TeV pp collisions, corresponding to an integrated luminosity of 36 pb^{-1}, recorded by the CMS experiment at the LHC. The observed forward energy depositions, their correlations, and the central charged-particle multiplicities are not well described by the available non-diffractive soft-hadron production models. A study of about 300 events with no significant energy deposited in one of the forward calorimeters, corresponding to a pseudorapidity gap of at least 1.9 units, is also presented. An indication for a diffractive component in these events comes from the observation that the majority of the charged leptons from the W(Z) decays are found in the hemisphere opposite to the gap. When fitting the signed lepton pseudorapidity distribution of these events with predicted distributions from an admixture of diffractive (POMPYT) and non-diffractive (PYTHIA) Monte Carlo simulations, the diffractive component is determined to be $(50.0 \pm 9.3\ (\text{stat.}) \pm 5.2\ (\text{syst.}))\%$.

1 Introduction

At high energies, proton–proton reactions are generally described in terms of a two-component outgoing system, pp $\rightarrow XY$, where X is a state originating from a perturbative parton–parton interaction and Y consists of proton remnants carrying a large fraction of the total energy. The system Y represents the "underlying event" and consists of mostly low-transverse-momentum hadrons originating from parton showers, and non-perturbative multi-parton interactions. The latter are largely independent of the hard interaction, increase the particle multiplicity, and lead to correlations between the energy flows in the central and forward regions.

The currently available models of multi-parton interactions have mainly been tuned to minimum-bias data and to final states including jets with large transverse momentum (p_T), using the observed central charged-particle multiplicities and the transverse momentum spectra of hadrons that are not associated with the hard jets. Models for a detailed simulation of multi-parton interactions are under rapid development and new features, including diffractive components in the energy flow, are being extensively investigated. A recent detailed CMS study of the underlying event structure at central rapidities is given in [1].

The analysis of the underlying event structure and energy flow correlations in hard processes with colorless final states, such as pp $\rightarrow$ W(Z)$X \rightarrow \ell\nu(\ell\ell)X$, can provide insights into unexplored aspects of multi-parton interactions. In particular, processes with colorless final states allow a straightforward separation of the hard interaction and the underlying event. Correlations between the charged-particle multiplicity in the central rapidity range and energy depositions at large rapidities can give additional information about multi-parton interactions.

Furthermore, a fraction of these proton–proton interactions is expected to arise from single-diffractive (SD) reactions, where one of the colliding protons emerges intact from the interaction, having lost only a few percent of its energy. Such SD events may be ascribed to the exchange of vacuum quantum numbers (often called Pomeron exchange), which leads to the absence of hadron production over a wide region of rapidity adjacent to the outgoing proton direction. Experimentally, these large rapidity gaps will appear as regions of pseudorapidity devoid of detected particles.

Soft-diffractive events can be described in the framework of Regge theory (see, e.g., [2]). Hard-diffractive events, with

* e-mail: cms-publication-committee-chair@cern.ch

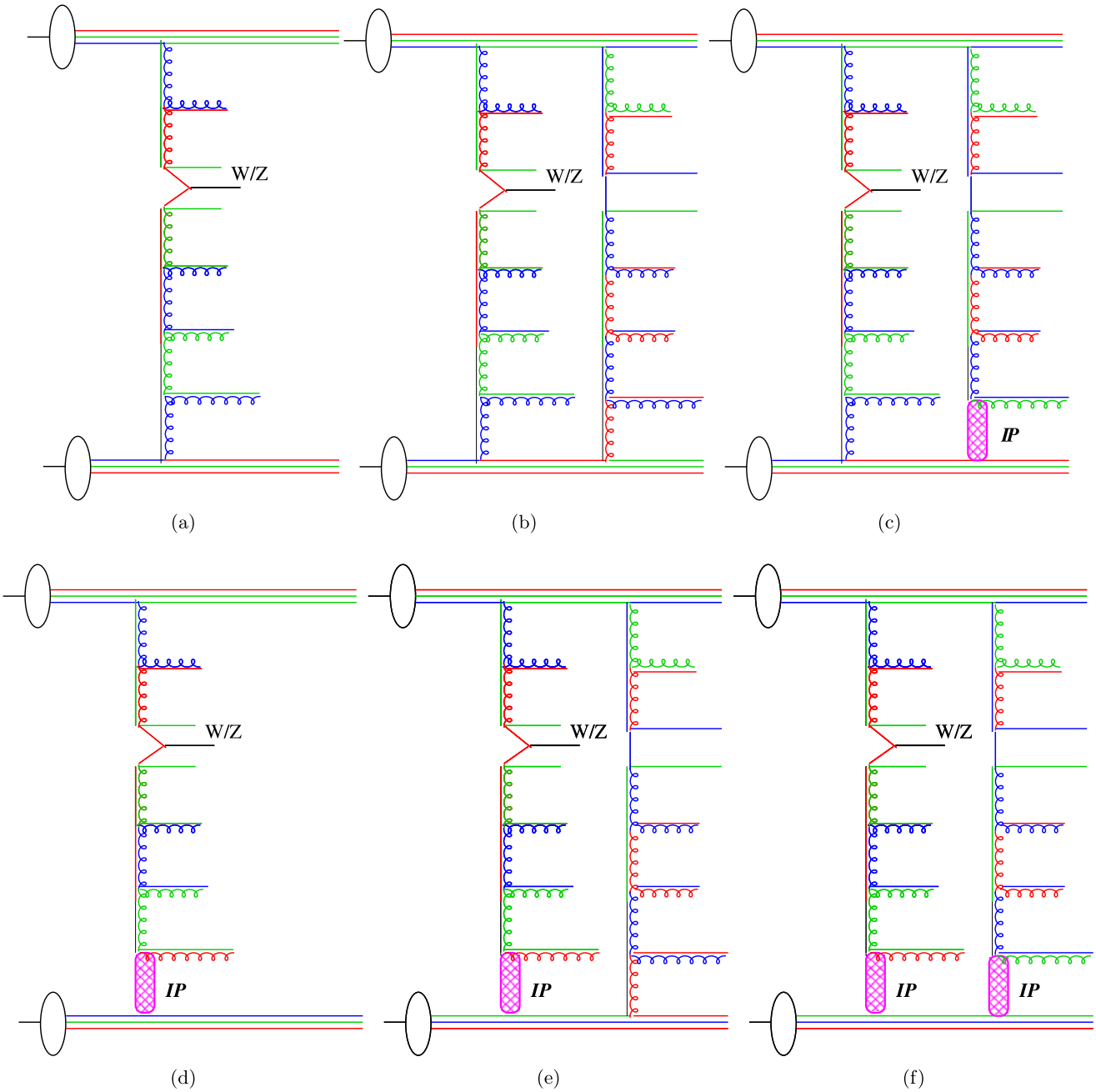

Fig. 1 Sketches of the process pp → W(Z)X, where a W(Z) boson is produced in the hard interaction, combined with contributions from multi-parton interactions, with and without a diffractive component. The *curly and straight lines* are for gluons and quarks, respectively, unless indicated (W/Z). The symbol $\mathbb{P}$ indicates the exchange of a state with the quantum numbers of the vacuum (Pomeron). (**a**) shows the standard hard interaction; (**b**) the same process with additional multi-parton interactions; (**c**) the hard process accompanied by multi-parton interactions containing a diffractive component; (**d**) the hard-diffractive production of a W(Z) boson; (**e**) the hard-diffractive W(Z) production with multi-parton interactions, and (**f**) the hard-diffractive W(Z) production with multi-parton interactions containing a diffractive component. In the latter case, the diffractive component of the multi-parton interaction does not necessarily couple to the same proton as in the hard process (not shown here)

the production of jets, heavy flavors, or W/Z bosons, have been observed at the SPS, HERA, and the Tevatron [3–8]. For electron-proton hard-diffractive interactions, a factorization theorem has been proven [9], allowing the introduction of diffractive parton distribution functions (dPDFs). In hadron-hadron diffractive interactions, factorization is however broken by soft multi-parton interactions [10, 11], which fill the large rapidity gap and reduce the observed yields of

hard-diffractive events. Such interactions are not yet simulated in the currently available Monte Carlo (MC) generators, and the reduction in the large rapidity gap hard-diffraction cross section is quantified by a suppression factor, the so-called rapidity gap survival probability. At the Tevatron, the observed hard-diffractive yields relative to the corresponding inclusive processes are approximately 1%. A recent study by CDF [12] indicates that the fractions of W and Z bosons produced diffractively are $(1.00 \pm 0.11)\%$ and $(0.88 \pm 0.22)\%$, respectively.

The standard picture of W or Z boson production via hard parton–parton scattering is shown in Fig. 1a and combined with a multi-parton interaction in Fig. 1b. According to this picture, large rapidity gap events can only arise from multiplicity fluctuations. Figure 1c shows standard W(Z) production accompanied by multi-parton interactions with a diffractive component. Hard-diffractive production (Fig. 1d) leads to a large rapidity gap. Such contributions would result in almost unchanged central charged-particle multiplicity distributions with respect to Fig. 1b. However, a larger fraction of events with a relatively small energy deposition in the forward regions, and a smaller correlation of the energy flow in the central and forward regions, could be expected. The diffractive production mechanism with multi-parton interactions is shown in Fig. 1e. In this case, large rapidity gap events only survive if the multi-parton component is small. Finally, Fig. 1f indicates a possible combination of W(Z) production mechanisms with a diffractive component in both the hard process and the multi-parton interaction.

This paper presents an analysis of the underlying event structure and of events with a pseudorapidity gap of more than 1.9 units (in the following, referred to as LRG events for simplicity) in the processes $pp \to WX$ and $pp \to ZX$, in 7 TeV pp collisions at the Large Hadron Collider (LHC), and recorded in 2010 with the Compact Muon Solenoid (CMS) detector. A data sample corresponding to an integrated luminosity of 36 pb^{-1} has been analyzed. Final states of the type WX and ZX are identified by the detection of electrons and muons with large transverse momentum p_T. The underlying event structure is analyzed in terms of (i) the charged-particle multiplicity at central rapidities, (ii) the forward energy flow, and (iii) the correlations between these observables. The observed LRG events are expected to be sensitive to a diffractive production component.

The paper is structured as follows: after giving a short description of the models for inclusive and diffractive vector–boson production in pp collisions (Sect. 2) and the CMS detector (Sect. 3), the selection of W and Z bosons with leptonic decays, the rejection of pileup events, and the energy measurement in the forward calorimeters are described in Sect. 4. Section 5 summarizes the analysis of the underlying event structure in WX and ZX events in terms of the observed charged-particle multiplicity, the energy depositions in the forward calorimeters, and their correlations. The analysis of events with a LRG signature is discussed in Sect. 6.

2 Modeling of the underlying event structure in W and Z events

The simulation of non-diffractive processes, including multiple overlaid events within the same bunch crossing ("pile-up"), was performed using the PYTHIA 6.420 and PYTHIA 8.145 event generators [13, 14] with different tunes [15] for the underlying event structure and the multi-parton interactions. Several tunes were used for the simulation of the underlying event structure in W and Z events. In particular, the tunes developed before data from the LHC could be used were PYTHIA6 D6T [16], Pro-Q20 [17], Pro-PT0 [17], and P0 [18]. The newer tunes PYTHIA6 Z2 [19] and the PYTHIA8 2C [20] include already some information from the LHC data. It is relevant for the discussion in Sect. 5 that the older D6T and Pro-Q20 tunes are associated with virtuality-ordered showers, while the newer ones, P0, Pro-PT0, Z2, and 2C, are associated with p_T-ordered showers. As shown in the recent CMS measurement of the underlying event structure Ref. [1], the Z2 tune provides a reasonably good description of the data in minimum-bias events.

Using the average instantaneous luminosity for each running period (discussed below), an average number of soft pileup minimum-bias MC events were superimposed on the simulated hard-interaction events. As discussed in detail in Sect. 5, the predicted pileup contribution to the forward energy flow from the simulation was found to be in good agreement with the one from a dedicated unbiased data sample.

The W and Z production cross sections were calculated using leading-order (LO) matrix elements for the process $q\bar{q} \to W(Z)$, convolved with the CTEQ 6.6 parton distribution functions (PDFs) [21]. Effects from higher-order QCD corrections were approximated with parton showers from the initial and final-state partons.

Diffractive W and Z production was simulated with the POMPYT 2.6.1 [22, 23] event generator. The hard processes responsible for the production of W and Z bosons were identical to those in non-diffractive models. For the simulation of diffractive processes, the dPDFs (fit B) measured by the H1 experiment at HERA were used [6, 24]. This generator does not simulate multi-parton interactions or the ensuing rapidity gap survival probability.

3 Experimental apparatus

A detailed description of the CMS experiment can be found elsewhere [25]. The coordinate system has the origin at the nominal interaction point. The Z-axis is parallel to the anticlockwise beam direction; it defines the polar angle θ and

the pseudorapidity $\eta = -\ln(\tan(\theta/2))$. The azimuthal angle ϕ is measured in the plane transverse to the beam, from the direction pointing to the center of the LHC ring toward the upward direction.

The central feature of the CMS apparatus is a superconducting solenoid, of 6 m internal diameter. Within the field volume are the silicon pixel and strip tracker, the crystal electromagnetic calorimeter (ECAL), and the brass scintillator hadronic calorimeter (HCAL). Muons are measured in gaseous detectors embedded in the steel return yoke. The ECAL, HCAL, and muon detectors are composed of barrel and endcap sections. The calorimeter cells are grouped in projective towers, of granularity $\Delta\eta \times \Delta\phi = 0.087 \times 0.087$ radians at central rapidities. For forward rapidities the HCAL towers have a granularity of 0.174 radians in ϕ and are increasing as a function of η. Besides the barrel and endcap detectors, CMS has extensive forward calorimetry. The forward hadronic calorimeter (HF) consists of steel absorbers and embedded radiation-hard quartz fibers, which provide fast collection of Cherenkov light. The maximum pseudorapidity coverage is $2.9 < |\eta| < 5.2$, but because of small differences in the passive material at large values of $|\eta|$ between the real detector and the simulation, a fiducial coverage of $3.0 < |\eta| < 4.9$ is used.

4 Event selection procedure

4.1 Selection of W and Z events with decays to electrons and muons

The identification of W and Z bosons is based on the presence of isolated electrons and muons with high transverse momentum. The selection criteria are given below. A more detailed description of the lepton selection, the efficiencies, and the associated systematic uncertainties is given in [26].

Events are selected online by requiring a high-transverse-momentum electron or muon with thresholds depending on the run period and varying between 10 and 17 GeV for electrons and between 9 and 15 GeV for muons. Thus, a small fraction of $W \to \tau\nu$ or $Z \to \tau\tau$ events with leptonic decays of the τ is also included. The trigger efficiency for signal events with the selection conditions defined below is above 99% [26].

The offline selection of electrons is based on the matching of a reconstructed high-transverse-momentum track candidate with energy depositions in the barrel and endcap calorimeters; shower shape requirements are applied to these clusters. Electron candidates are required to have $|\eta| < 2.5$ and transverse momenta larger than 25 GeV. Electrons from photon conversions are rejected. In order to suppress background from jets, the electrons are required to be isolated using a cone in $\eta - \phi$ space around the electron direction with $\Delta R < 0.3$, where $\Delta R = \sqrt{\Delta\eta^2 + \Delta\phi^2}$ and $\Delta\eta$ and $\Delta\phi$ are the pseudorapidity and azimuthal angle difference between the electron and jet directions. The energy in the cone is calculated from the scalar sum of the transverse energies in the tracker and both calorimeters, and is required to be smaller than 10% of the lepton p_T. More details are given in Ref. [26].

Two algorithms are used to identify muons. One is based on the matching of a reconstructed high-transverse-momentum silicon tracker candidate with a track candidate found in the muon system. The second is based on a global fit to tracker and muon system hits. Muons in this analysis have to pass both selection algorithms. The reconstructed muon candidates are required to be at $|\eta| < 2.5$ and to have transverse momentum larger than 25 GeV. The isolation criteria are similar to the ones used for electrons, and details about the muon identification are given in Ref. [26].

Jets and the missing transverse momentum in the event are determined from the four-vectors of reconstructed particles, which are measured from the combination of the tracker and the calorimeter informations [27]. For jets, the anti-k_t algorithm with a cone size of 0.5 is used [28]. The transverse momentum of jets is required to be larger than 30 GeV with a pseudorapidity of $|\eta| < 2.5$.

An event is selected as a $W \to \ell\nu$ candidate if the following requirements are satisfied: (1) one isolated electron or muon with a transverse momentum greater than 25 GeV and $|\eta| < 1.4$; events with a second isolated electron or muon with a transverse momentum above 10 GeV are rejected; (2) the missing transverse momentum (ascribed to the neutrino) greater than 30 GeV; (3) the transverse mass $= \sqrt{2E_T(\nu)E_T(\ell) - 2\boldsymbol{p}_T(\nu)\cdot\boldsymbol{p}_T(\ell)}$ of the charged lepton and the neutrino greater than 60 GeV.

Likewise, the following conditions are imposed to select $Z(\gamma^*) \to \ell\ell$ (called Z in the following) candidates: (1) two isolated electrons or muons with opposite charge and each with a minimum transverse momentum of 25 GeV; (2) at least one lepton with $|\eta| < 1.4$; (3) the reconstructed invariant mass of the dilepton system between 60 and 120 GeV.

This selection resulted into essentially background-free W and Z event samples. The background for the W sample is estimated to be less than 1% and even smaller for the Z sample, independent of any additional requirements on the energies in the HF calorimeters.

The main features of the W and Z event samples are found to be insensitive to small variations of the selection criteria. In the following, no efficiency corrections are applied, and only direct comparisons to MC predictions are shown.

4.2 Pileup rejection and single-vertex selection of W and Z events

As mentioned earlier, there can be several simultaneous pp interactions in the same bunch crossing in addition to the

Table 1 Number of W and Z candidate events with a single primary vertex. The numbers are given for the total and the three data-taking periods of different instantaneous luminosities. The percentage of single-vertex events with respect to all selected W and Z candidates for that period is given in parentheses

Single-vertex events	$W \to e\nu$	$W \to \mu\nu$	$Z \to ee$	$Z \to \mu\mu$
Total	13995 (25.8%)	17924 (26.2%)	1749 (25.7%)	2924 (26.1%)
P I	1502 (55.0%)	1926 (53.0%)	188 (53.0%)	328 (56.8%)
P II	7961 (31.0%)	10524 (32.7%)	1018 (31.4%)	1718 (31.0%)
P III	4532 (17.6%)	5474 (17.3%)	543 (16.8%)	878 (17.2%)

selected W and Z events, the so-called pileup. As the number of bunches and the instantaneous luminosity increased steadily during the 2010 pp data taking, the analysis was affected by very different pileup conditions. For this analysis the data have been separated into three periods (P) with average instantaneous luminosities of $L_{\text{inst}} \leq 0.17\ \mu\text{b}^{-1}/\text{s}$ (P I), $0.17 < L_{\text{inst}} \leq 0.34\ \mu\text{b}^{-1}/\text{s}$ (P II), and $L_{\text{inst}} > 0.34\ \mu\text{b}^{-1}/\text{s}$ (P III), respectively. Assuming a total inelastic cross section of about 70 mb [29, 30], an instantaneous luminosity of $0.17\ \mu\text{b}^{-1}/\text{s}$ corresponds to an average of about one inelastic pileup event.

The selection efficiency for W and Z events is independent of the instantaneous luminosity. However, the charged-particle multiplicities and the energy depositions in the forward region of the detector (HF calorimeters), and thus especially the LRG signature, are strongly affected by the pileup (i.e., the gap is filled in).

The effects from pileup events for our analysis have been studied by means of zero-bias data samples where the only requirement was that of beams crossing in the detector. Such event samples were collected and analyzed for different instantaneous luminosities and the different periods. More details are given in Sect. 5.1.

In order to limit the consequences of pileup, events with more than one vertex are rejected. For this analysis a primary vertex, the W(Z)-vertex, is defined as the one which contains the lepton track(s). Events with additional vertices, formed by at least three tracks, are rejected. Details about the vertex reconstruction algorithm are given in Ref. [31]. The W-vertex z-position distribution is roughly Gaussian with a mean of 0.52 cm and a standard deviation of 5.9 cm.

The observed increase in the number of vertices has been studied using a zero-bias event sample and found to be in agreement with the number of pileup events expected on the basis of the luminosity increase (cf. Table 1). Pileup events can be categorized as hard and soft events. Hard pp pileup interactions have some detectable charged particles in the central region of the detector and are removed by the multiple-vertex veto. The soft component has little or no detectable transverse activity in the central region and does not result in reconstructed vertices.

The efficiency to reconstruct pileup vertices (including vertex splitting) has been determined from MC simulations of minimum-bias and $W \to e\nu$ events. Based on the pileup conditions in the 2010 data, the efficiency to detect pp pileup interactions was found to be essentially constant within ± 25 cm along the z direction of the nominal interaction point with an average of about 72%. The inefficiency essentially depends only on the amount of soft pileup interactions (e.g., events without detectable charged particles in the central region of the detector) in the MC simulation. The reconstruction efficiency for pileup vertices was found to be essentially independent for the different luminosity periods, as long as the vertices were separated by more than 0.1 cm. The corresponding inefficiency to detect the merged pileup vertex is estimated to be 3.3%. The uncertainties from the remaining soft pileup events on the results presented below are discussed in more detail in Sect. 5.1.

The numbers of single-vertex W and Z events are summarized in Table 1. The single-vertex event yields, compared to the inclusive event yields, decrease with increasing instantaneous luminosity and are in agreement with the expected numbers of vertices from the simulation, assuming Poisson distributions.

5 Central charged-particle multiplicity and forward energy flow

The observables used to study the underlying event structure in W and Z events are the charged-particle multiplicity in the central detector, the energy depositions in both HF calorimeters (in the following designated as HF+ and HF− depending on the sign of the corresponding η coverage), and the correlations between them. In the following, only the distributions for $W \to \ell\nu$ events are discussed. No significant differences are observed between W events selected with decays to electrons or muons. The same analysis has been performed on the $pp \to ZX$ data sample and consistent results are obtained.

For the studies described below, the charged-particle multiplicity is measured in the range $|\eta| < 2.5$ for track momentum thresholds of $p_T > 0.5$ GeV and $p_T > 1.0$ GeV, excluding the tracks associated with W decays. Additionally,

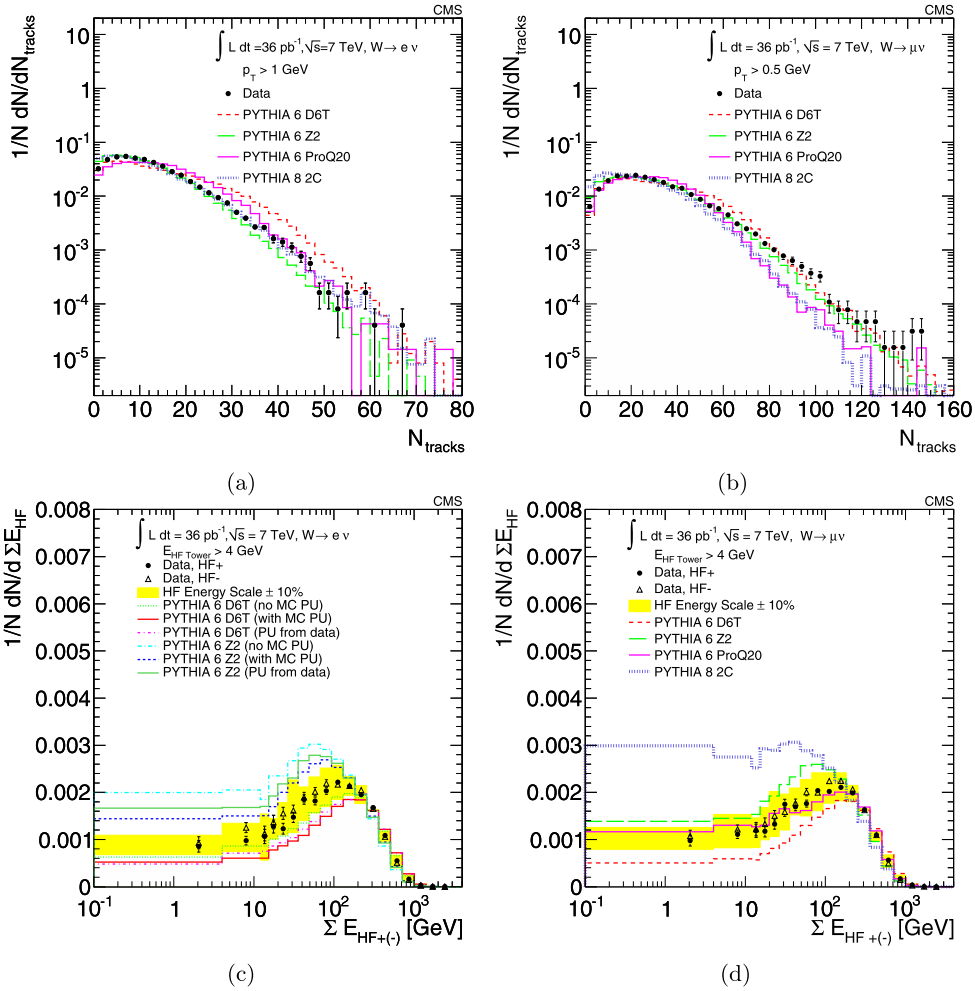

Fig. 2 The charged-particle multiplicities and the summed HF+ and HF− energy distributions in (**a**) and (**c**) $W \to e\nu X$ and (**b**) and (**d**) $W \to \mu\nu X$ candidate events are shown for data and MC simulations, including pileup, with different tunes for the underlying event. The uncorrected charged-particle multiplicities are shown separately (only for reasons of simplicity) for electron- and muon-tagged W events, for two thresholds on track transverse momenta of (**a**) $p_T > 1.0$ GeV and (**b**) $p_T > 0.5$ GeV. The band shown for the HF energy distributions indicates the uncertainty related to a ±10% HF energy scale variation. The effects of the pileup on the MC simulation can be seen in (**c**) where the MC HF energy distributions are shown with pileup taken either from data or from the MC simulation and without pileup

in order to study the underlying event structure, events with central jet activity ($p_T > 30$ GeV, $|\eta| < 2.5$) are excluded from the multiplicity plots.

A detailed study of the pion track reconstruction within the acceptance of the tracker [31] determined that the efficiency rises from about 88% at a p_T of 0.5 GeV to about 95% for p_T between 1–10 GeV. Above 10 GeV, the efficiency decreases slowly to about 90% at 50 GeV. Furthermore, it was shown that the hadron track reconstruction efficiency in the data agrees within 1–2% with the one in the MC simulation. The total systematic uncertainty of the tracking efficiency was estimated to be less than 3.9%. The observed charged-particle multiplicities, excluding the lepton(s) from the W(Z) decays, vary between 0 and about 50, with an average of 11 and an r.m.s. of 8.2 for $p_T > 1.0$ GeV. About twice as many tracks are found with the lower threshold, $p_T > 0.5$ GeV, and about 0.15% of the events have more than 100 tracks. Nearly identical charged-particle multiplicity distributions are observed in electron- and muon-tagged events with the same p_T thresholds. The charged-particle multiplicity distribution for $W \to e\nu$ events is shown in Fig. 2a for tracks with $p_T > 1.0$ GeV, and for $W \to \mu\nu$ events with for $p_T > 0.5$ GeV in Fig. 2b. The corresponding distributions for $W \to e\nu$ with $p_T > 0.5$ GeV and $W \to \mu\nu$ with $p_T > 1.0$ GeV are consistent with the displayed distributions in Figs. 2a and 2b.

The PYTHIA8 generator with tune 2C provides the best overall description for the higher track p_T threshold, and PYTHIA6 with tune Z2 provides a reasonable description for both track p_T thresholds. However, both PYTHIA8 2C and PYTHIA6 Z2 predict too many events with very small charged-particle multiplicities. The PYTHIA6 D6T tune predicts a harder-p_T spectrum for hadrons in the underlying event and thus a larger multiplicity in the case of the higher threshold. The Pro-Q20 tune of PYTHIA6 significantly underestimates the event yields with very high multiplicities (Fig. 2b).

The energy deposition in the HF+ and HF− calorimeters is determined from the sum of individual calorimeter towers with an energy threshold of 4 GeV, corresponding to a minimum transverse momentum of 0.07–0.4 GeV. The uncertainty on the energy scale of the HF calorimeter was estimated to be about ±10% (for details see [27]). This uncertainty was taken into account by a ±10% scaling of the

Table 2 Mean energy depositions and tower multiplicities in each HF for single-vertex W events from the three running periods with different instantaneous luminosities

Mean energy [GeV]	$pp \to W(\to e\nu)X$	$pp \to W(\to \mu\nu)X$
HF+/HF−, P I	298.3/284.7	295.7/286.4
HF+/HF−, P II	308.2/296.6	313.0/295.7
HF+/HF−, P III	322.6/313.6	329.6/310.8
Average tower multiplicity		
HF+/HF−, P I	29.2/28.5	29.4/28.5
HF+/HF−, P II	30.5/29.6	30.9/29.6
HF+/HF−, P III	32.1/31.2	32.7/31.2

single-tower energy, resulting in new estimates of the total energy deposition in HF for the data, while keeping the MC unchanged. In Fig. 2 and all the following figures, the data points are plotted in the center of the corresponding bins, and the corresponding systematic uncertainty for the energy measurement in the HF is shown as a band. This uncertainty is much larger than the 3.5% difference between the reconstructed energy distributions in the HF+ and HF− calorimeters (cf. Table 2).

The observed HF energies vary between 0 GeV (i.e., no HF tower with an energy above 4 GeV) and more than 2 TeV. Only a few events have an energy deposition above 2 TeV (about 0.05% for electrons and muons combined) and the highest energy deposition is 2.7 TeV. All events with high-energy depositions also have large tower multiplicities. The average energies observed in HF+ and HF− are measured in 11 HF rings of calorimeter towers, each covering approximately a $\Delta|\eta|$ range of 0.175. The difference between the average energy deposition per ring (η bin) in the data and the different MC tunes is consistent for all tower rings. The average energy deposited per $|\eta|$ ring predicted by the D6T (Z2) tune is too large (too small), while the Pro-Q20 tune provides a very good description of the data.

The distributions of the total HF+ and HF− energy sums ($E_{\mathrm{HF}+(-)}$) are shown in Fig. 2c for the data and the PYTHIA6 D6T and Z2 tunes, with and without pileup (PU) in $W \to e\nu$ events. In order to take into account effects not included in the simulation (e.g., beam–gas interactions), the soft pileup contribution obtained from the zero-bias data is added to the MC simulation without pileup. It can be seen that the pileup contribution, as determined from the data, is, compared with the energy scale uncertainty, found in reasonable agreement with the one obtained from the luminosity-dependent MC simulation. Therefore, in the following analysis and all shown distributions, the pileup contribution is estimated from the MC simulation, using events simulated with PYTHIA6 D6T. Figure 2d shows the HF+ and HF− energy sums for $W \to \mu\nu$ events and for several different MC tunes of the underlying event.

The mean values of the reconstructed HF energy and the tower multiplicities are given in Table 2, again for the three different instantaneous luminosity periods and separately for $W \to e\nu$ and $W \to \mu\nu$ events.

The average HF energy deposition, averaging the energy deposits in the HF+ and HF− calorimeters, in the data is 310 GeV, with an r.m.s. of 235 GeV. On average, about 30 towers with more than 4 GeV are reconstructed in each HF calorimeter. The statistical uncertainties of the mean energy values (mean tower multiplicities), estimated from the r.m.s. of the distribution, amount to less than ± 5 GeV (± 0.4) in the data and even smaller in the MC simulation. The corresponding mean value obtained with PYTHIA6 D6T, including the HF energy depositions from simulated pileup, is 370 GeV, with a tower multiplicity of 35. The PYTHIA6 Z2 tune predicts a mean energy deposition of 270 GeV and a tower multiplicity of 27, whereas using the Pro-Q20 tune results in a simulated energy deposition of 311 GeV and a tower multiplicity of 29 towers, similar to the data.

As can be seen from Figs. 2c and 2d, besides the Pro-Q20 tune, none of the MC models considered provide a good description of the HF energy distribution observed in the data. For energy depositions between 10 and 150 GeV, large differences between the data and different tunes are observed. In particular, the number of events in the data is about 30 to 50% higher than predicted by the D6T tune, and 50% lower than predicted by the Z2 tune. For simplicity, the older P0 and Pro-PT0 tunes are omitted from the following more detailed studies.

In total, 287 W and Z events with no individual tower energy deposition above 4 GeV in one HF calorimeter, are observed. These events are defined as LRG events, i.e., events with "zero" energy depositions, and are discussed in detail in Sect. 6.

5.1 Soft pileup events and HF energy distributions

The observed mean energy values in the HF increased by about 10 ± 5 GeV from period I to period II and by about 15 ± 5 GeV from period II to period III (cf. Table 2), both in $W \to e\nu$ and $W \to \mu\nu$ events. This increase of HF energy depositions is interpreted as arising from soft pileup events, not identified by the vertex finder. A similar increase of the mean energy deposition in HF is also seen in the MC simulations, when events with and without pileup are compared.

The properties of such soft pileup events have been studied with the zero-bias data samples, where the only requirement was that of beams crossing in the detector, taken during the different running periods. In events from this sample with zero reconstructed vertices, three classes of events can be identified: (1) events with no energy deposition in either HF (hereafter referred to as quasi-elastic pp-scattering), (2) events with zero energy in only one of the HF calorimeters and non-zero energy in the other (soft scattering with a

LRG signature), and (3) events with non-zero energy depositions in both HF calorimeters (soft inelastic pp-scattering).

The contributions of beam-gas events and other beam-related backgrounds to the HF energy dispositions were studied in randomly triggered events with non-colliding beams and were found to be negligible.

The relative fraction of quasi-elastic pp-scattering event candidates in the zero-bias samples decreases from about 50% in period I to 20% in period III, while the fraction of soft inelastic events increases from about 15% in period I to 40% in period III. The fraction of soft events with a LRG signature of about 40% is roughly constant across the three luminosity periods.

In conclusion, soft pileup events, not identified by the single-vertex requirement, can have an important effect on the HF energy distributions and on LRG events in particular. As discussed below, their contribution is well modeled by the MC simulations.

5.2 Correlations of the forward energy flow and the central charged-particle multiplicity

In the following, the correlation between the central charged-particle multiplicity and the forward energy flow is measured in the data and compared to MC models. For this study, events with energy depositions in the HF− calorimeter of 20–100 GeV (low), 200–400 GeV (medium), and above 500 GeV (high) are selected. The central charged-particle multiplicity distributions with track p_T thresholds of 1 GeV (for $W \to e\nu$ events) and 0.5 GeV (for $W \to \mu\nu$ events) are shown in Fig. 3, while the HF+ energy distributions for the three HF− energy intervals are shown in Fig. 4 (for $W \to e\nu$ and $W \to \mu\nu$ events).

The charged-particle multiplicity distributions for the medium HF− energy range (Figs. 3c and 3d) are described reasonably well by the PYTHIA6 D6T and Z2 tunes. The agreement between the data and the D6T tune is poorer when a 1 GeV track p_T threshold is applied. For the low HF energy range (Figs. 3a and 3b), the D6T tune fails to describe the charged-particle multiplicity distribution, whereas the Z2 tune is in good agreement with the data, after applying a 0.5 GeV track p_T threshold. Finally, when requiring a large HF energy deposition (Figs. 3e and 3f), the Z2 tune provides a good description, whereas the D6T tune overestimates the charged-particle multiplicity.

The HF+ distributions for the medium HF− energy interval (Figs. 4c and 4d) are in better agreement with the predictions of the various tunes than the inclusive HF distributions (Figs. 2c and 2d). On the other hand, when requiring a low HF− energy deposition, the HF+ energy distribution is poorly modeled by all MC tunes (Figs. 4a and 4b). Finally, for events with high-energy depositions in HF−, the PYTHIA8 generator, which in the inclusive case underestimates the rate of events with large HF− energy depositions, provides a good description of the energy distribution in HF+. Conversely, all other tunes predict more events with large HF+ energy than observed in the data (Figs. 4e and 4f).

Figure 5 shows the minimum and maximum energy depositions per event in the HF+ and HF− calorimeters for the data and the various MC tunes. In comparison to Fig. 2, the differences between the data and all available MC tunes are somewhat enhanced.

5.3 Interpretation of the observed HF energy and charged-particle multiplicity correlations

As seen in the previous section, the energy distributions in the two HF calorimeters and the central charged-particle multiplicities are strongly correlated: large energy depositions in one of the HF calorimeters correspond to large energy depositions in the other HF calorimeter, as well as to an increase in the central charged-particle multiplicity. Such correlations are also predicted by the various MC tunes, though with very different strengths. Our observations can be summarized as follows:

D6T tune The inclusive distribution of charged-particle multiplicities, with a minimum p_T of 0.5 GeV, is reasonably well described, whereas raising this threshold to 1 GeV leads to an overestimation of the event rate with large multiplicities. Furthermore, on average much-larger HF energy depositions are predicted than observed. When selecting events with small energy depositions in the HF, the fraction of events in the data is 30–50% larger than predicted by the D6T tune. In terms of correlations, the D6T tune provides a reasonable description only for the charged-particle multiplicity in the medium HF− energy interval (track p_T threshold of 0.5 GeV) and for HF+ energy distribution corresponding to the low HF− energy bin.

Z2 tune Overall, the Z2 tune provides a very good description of the inclusive charged-particle multiplicities, but predicts too many events with very low charged-particle multiplicities. Concerning the HF energy distributions, too many events with low-energy depositions are predicted. The correlations between charged-particle multiplicity and HF− energy are well described. The HF+ energy distribution obtained for the low HF− energy interval is badly modeled, with the MC prediction much higher than the data at low energies. However, the correlations are well described for the higher HF− energy intervals.

Pro-Q20 tune This tune provides the best description of the HF energy distributions and the charged-particle multiplicities with the $p_T > 0.5$ GeV threshold. However, the inclusive charged-particle multiplicity for the $p_T > 1.0$ GeV threshold is not well described, though still closer to the

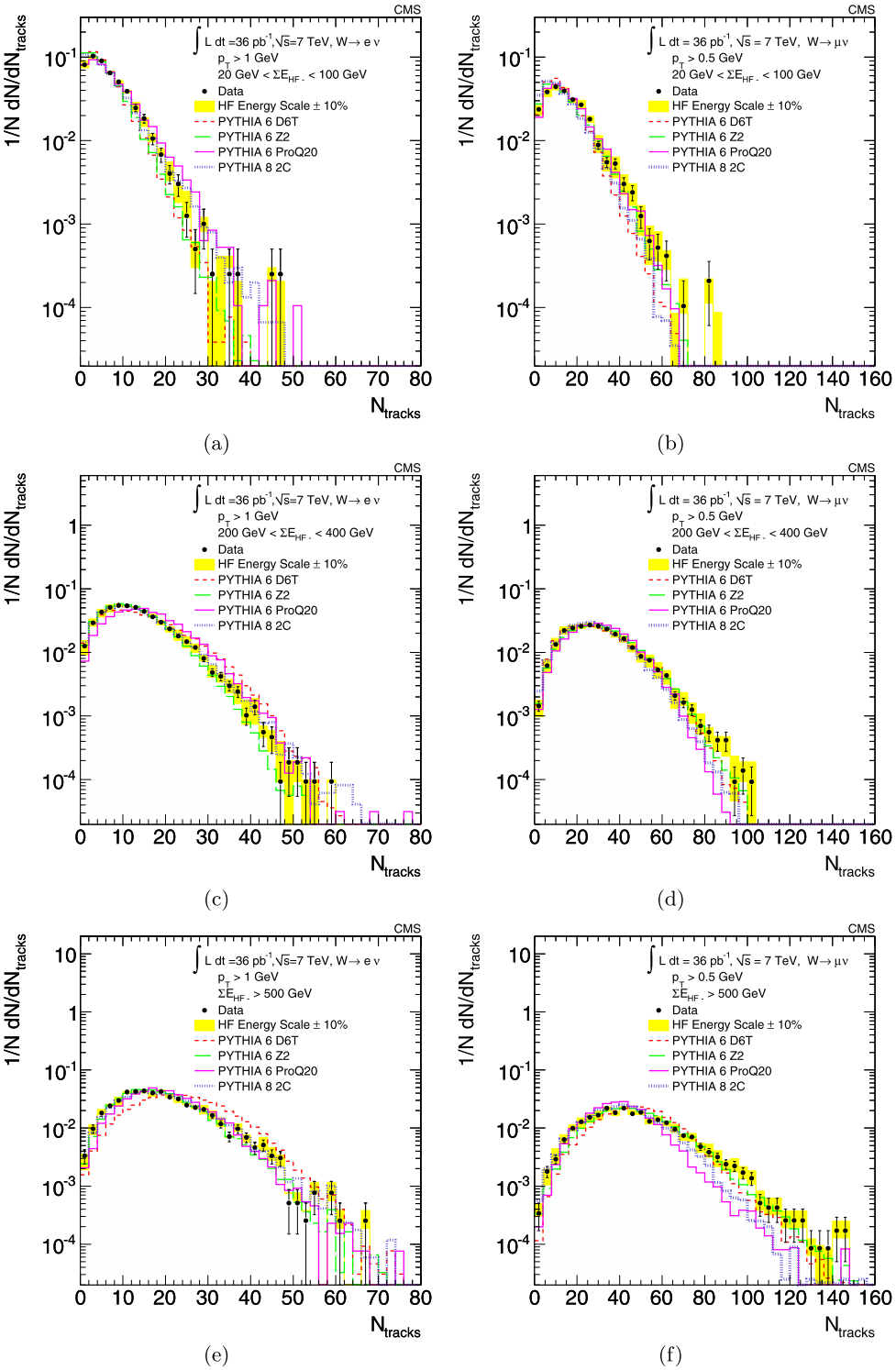

Fig. 3 Charged-particle multiplicity distributions in the data and from MC simulations with different tunes, for the three HF− energy intervals of (**a**) and (**b**) 20–100 GeV, (**c**) and (**d**) 200–400 GeV, and (**e**) and (**f**) >500 GeV. The *plots in the left column* are for $pp \to W^{\pm}X \to e^{\pm}\nu X$, for tracks with $p_T > 1.0$ GeV, and *those in the right column* for $pp \to W^{\pm}X \to \mu^{\pm}\nu X$, for $p_T > 0.5$ GeV (different scales are used for the x-axes)

data than the D6T tune. In terms of correlations, the central charged-particle multiplicities are reasonably well described, though the fraction of events with large multiplicity and a large HF− energy deposition is underestimated. Furthermore, too many events with low-energy depositions in HF+ are predicted when a low-energy deposition in HF− is selected. For the other HF− energy bins this tune provides a good description of the data.

PYTHIA8 *2C tune* In the inclusive case, this tune predicts too many events with low HF energy depositions, whereas the central charged-particle multiplicity distributions are

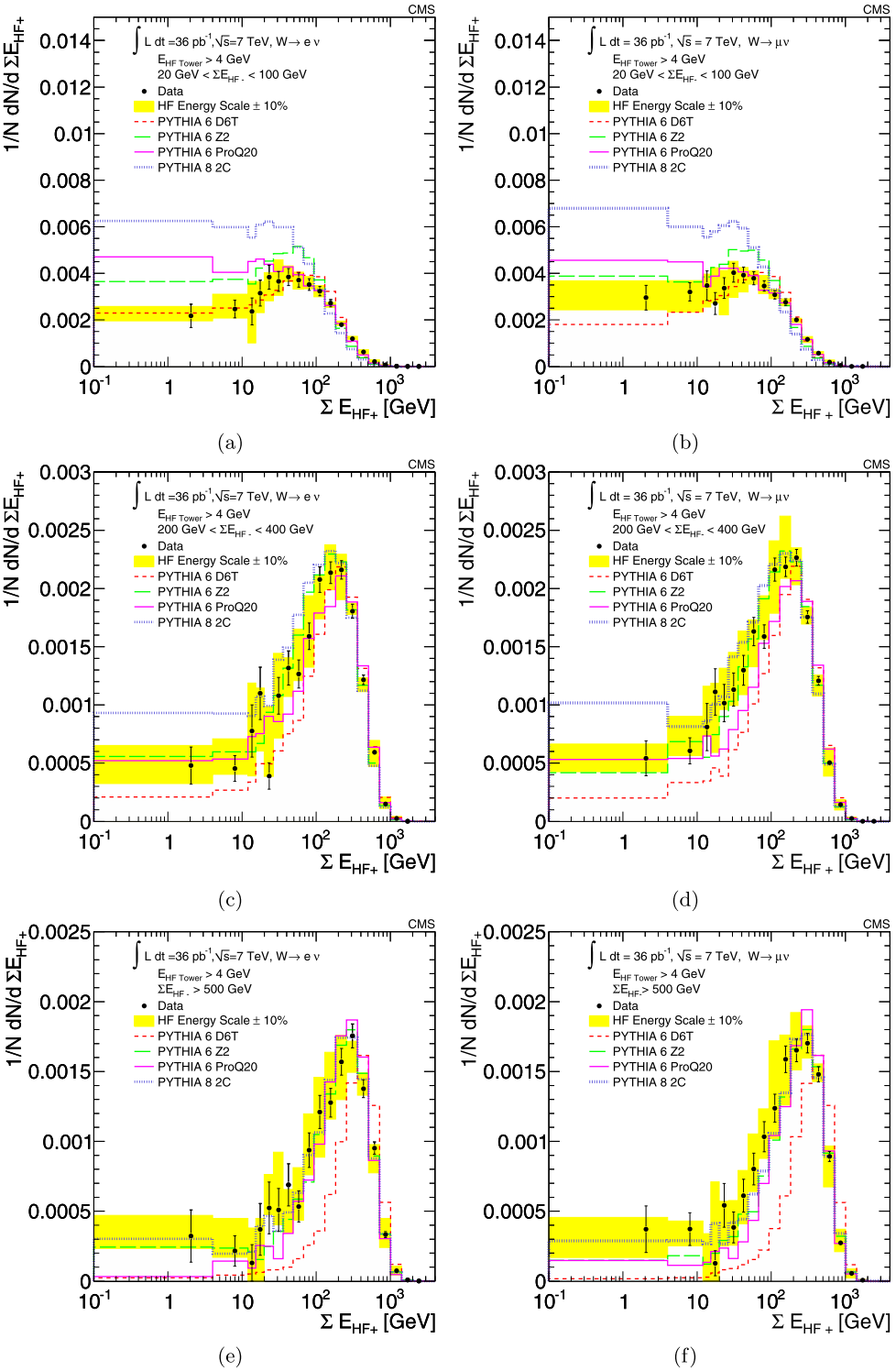

Fig. 4 Energy distribution in the HF+ calorimeter, shown for different HF− energy intervals (**a**) and (**b**) 20–100 GeV, (**c**) and (**d**) 200–400 GeV, (**e**) and (**f**) >500 GeV, for data and different MC tunes. *In the left column*, the plots are shown for $pp \to WX \to e\nu X$ events and *in the right column*, for $pp \to WX \to \mu\nu X$

well described. The HF+ energy distributions for the cases of low and medium HF− energy intervals are shifted towards lower values compared to data, whereas for the high-energy bin good agreement is found.

In summary, none of the analyzed MC tunes provides an overall consistent and reasonable description of the inclusive charged-particle multiplicities and the HF energy distributions in the W data sample, as well as correlations between them. It follows that the tunes, which provide a reasonable description of the underlying event structure for central rapidities in jet events, as presented in [1], require substantial modifications to describe the W data presented here. Simi-

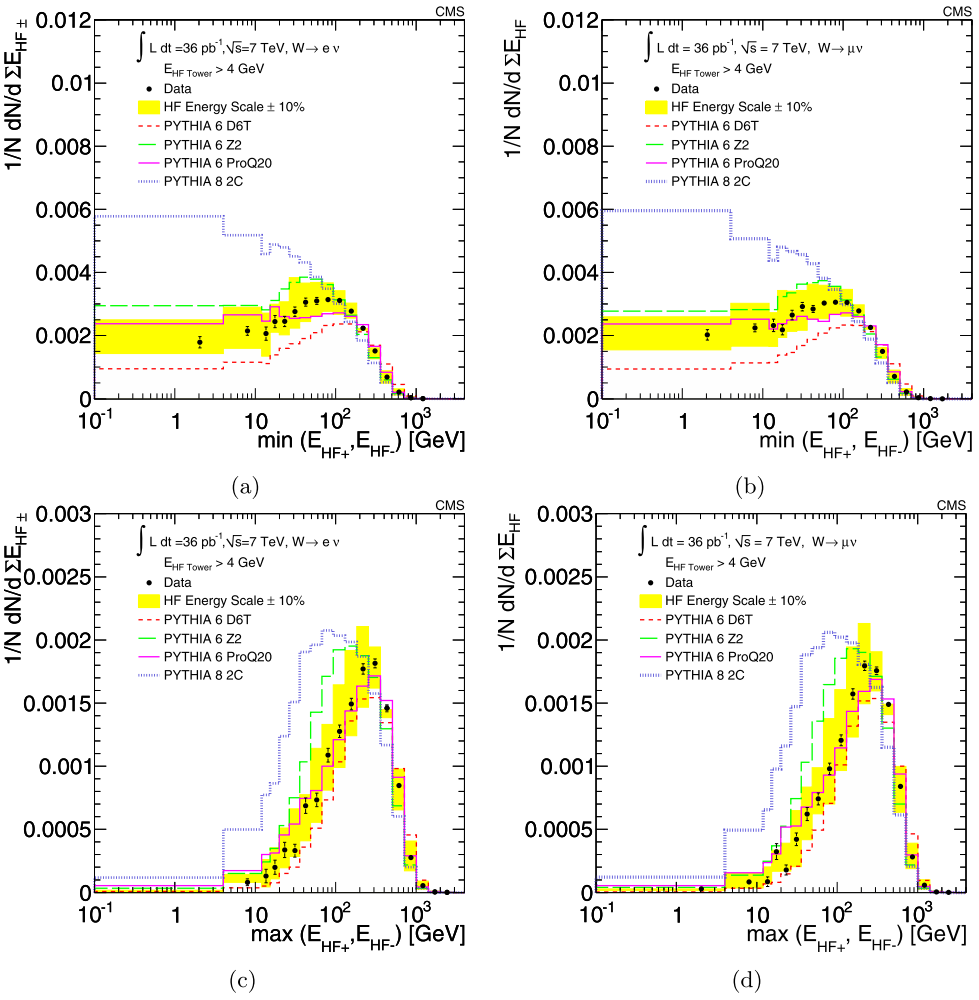

Fig. 5 HF energy distributions in $W \to e\nu X$ (*left column*) and $W \to \mu\nu X$ (*right column*) events for data and different MC tunes. The plots (**a**) and (**b**) show the minimum (min (E_{HF+}, E_{HF-})) and (**c**) and (**d**) the maximum (max (E_{HF+}, E_{HF-})) of the energy depositions per event in the HF+ and HF− calorimeters

lar, though statistically less significant results were obtained from the corresponding Z event samples.

6 W and Z events with large pesudorapidity gaps

As the next step, the subset of W and Z events with a single primary vertex and a LRG signature was analyzed.

A LRG event was defined by the requirement that none of the calorimeter towers had a measured energy of more than 4 GeV in at least one of the HF calorimeters, corresponding to a pseudorapidity interval of 1.9 units. This subset of events may be enhanced by a diffractive W/Z production mechanism.

6.1 Observed number of LRG events

Table 3 shows the observed LRG event yields and their ratio to the number of inclusive W and Z single-vertex events for the three luminosity periods. This ratio decreases by roughly a factor of 2 to 4 when going from period I to period III.

Table 3 Number of LRG events with a single vertex and their percentage relative to all selected W and Z events, for the three different luminosity periods and their total

	$W \to e\nu$	$W \to \mu\nu$	$Z \to ee$	$Z \to \mu\mu$
Total	100 (0.71%)	145 (0.81%)	19 (0.80%)	23 (0.79%)
P I	17 (1.13%)	31 (1.61 %)	7 (2.7%)	3 (0.91%)
P II	57 (0.72%)	91 (0.86 %)	9 (0.59%)	16 (0.93%)
P III	26 (0.57%)	23 (0.42%)	3 (0.55%)	4 (0.46%)

The decrease can be explained by the HF energy depositions coming from soft pileup events. As discussed in Sect. 5.1 (cf. Fig. 2c), adding pileup to the Monte Carlo simulation shifts some of the LRG events to the class of low-energy depositions in the HF.

The inefficiency to detect a vertex in an event with forward energy deposition depends on the instantaneous luminosity and is estimated from zero-bias events (Sect. 5.1). After correcting the observed number of LRG events in the data for pileup effects, using data, a constant fraction of LRG events, relative to the total number of W and Z events with

Table 4 Percentage of LRG events in single-vertex W and Z events, using a pileup correction determined from data, for the entire dataset and the three different luminosity periods. Only the statistical uncertainties are given; the dominant systematic uncertainty from the HF energy scale is about ±26%

	$W \to e\nu$	$W \to \mu\nu$	$Z \to ee$	$Z \to \mu\mu$
Total	$1.37 \pm 0.14\%$	$1.50 \pm 0.13\%$	$1.73 \pm 0.43\%$	$1.49 \pm 0.31\%$
P I	$1.68 \pm 0.41\%$	$2.39 \pm 0.43\%$	$5.52 \pm 2.08\%$	$1.36 \pm 0.78\%$
P II	$1.27 \pm 0.17\%$	$1.54 \pm 0.16\%$	$1.57 \pm 0.52\%$	$1.65 \pm 0.41\%$
P III	$1.53 \pm 0.30\%$	$1.12 \pm 0.23\%$	$1.47 \pm 0.85\%$	$1.22 \pm 0.61\%$

a single primary vertex, is found for the three instantaneous luminosity periods. The corrected fraction of LRG events is given in Table 4. The uncertainties on this correction are small compared to the statistical errors and to the ±10% energy scale uncertainties of the HF calorimeters (for details see [27]). Indeed, this energy scale variation is the dominant systematic uncertainty for the estimated fraction of LRG events in the data, resulting in a change of about ±26% when varying the tower energy threshold between 3.6 and 4.4 GeV.

Combining the results obtained with electrons and muons, the percentage of W and Z events with LRG signature is $(1.46 \pm 0.09\ (\text{stat.}) \pm 0.38\ (\text{syst.}))\%$ and $(1.57 \pm 0.25\ (\text{stat.}) \pm 0.42\ (\text{syst.}))\%$, respectively. In comparison, as can be seen from Figs. 2 and 5, the fraction of W LRG events predicted with the PYTHIA6 Z2 and Pro-Q20 and the PYTHIA8 2C tunes are larger than observed in the data. In contrast, for the D6T tune the number of LRG events is smaller than in the data.

6.2 Jet activity in W/Z events with a LRG signature and search for exclusive W/Z production

A further subset of W and Z events are those that show some jet activity, using the particle-flow algorithm with a cone size of 0.5. We find $(11.1 \pm 0.2)\%$ of the selected W and Z events with a single vertex contain at least one reconstructed jet with a transverse momentum above 30 GeV and $|\eta| < 2.5$. Taking the subsample of 100 identified $W \to e\nu$ events with a LRG signature, 8 events are found with one or more jets above a 30 GeV threshold. The corresponding numbers for the muon channel are 145 identified LRG events and 8 of them with at least one jet. Thus, we find that $(6.5 \pm 1.6)\%$ of the LRG events have jet activity, which is smaller (but still consistent) with the fraction of events with jets observed in the inclusive W sample. No other particular features of the events with jet activities, when compared to the MC simulations, are observed.

Another potentially interesting class of LRG events consists of W and Z events with essentially no activity besides that from the vector–boson decays. Such candidate exclusive events are selected with the requirement that both HF calorimeters fulfill the LRG condition and that no particle-flow object besides the lepton(s) is reconstructed in the central detector, above a transverse momentum threshold of 0.5 GeV. For the electron selection no such events are found. In the muon case, 2 W and 2 Z event candidates with zero energy in both HF calorimeters are found. All four events have some reconstructed tracks in the central detector. The number of observed events is consistent with expected number of non-exclusive W and Z events predicted from the MC simulations.

6.3 Size of the pseudorapidity gap and central gaps

For the study of events with large pseudorapidity gaps an interesting parameter is how far the size of the gap extends into the central detector. One might intuitively expect that the ratio of diffractive signal events compared to background from multiplicity fluctuations, would become larger when the gap size increases into the central detector. This intuitive view is confirmed when comparing diffractive W events simulated with POMPYT, where the decrease in event yields with increasing gap size is much smaller than in the different non-diffractive MC models.

Obviously, the definition of the gap is ambiguous, as the meaning of zero activity or zero energy depositions depends on the experimental criteria for the detection of particles in the data and in the MC simulation. For this study the size of the pseudorapidity gap was determined by using particle-flow objects with a minimum energy of 1.5 GeV for $|\eta| < 1.5$ (barrel), 2 GeV for $1.5 < |\eta| < 2.85$ (endcaps), and 4 GeV for $|\eta| > 2.85$ (HF calorimeters). For charged particle-flow candidates a minimum transverse momentum of 0.5 GeV was required. The largest ($\eta_{\max}$) and smallest ($\eta_{\min}$) observed pseudorapidity values of the particles are used to determine the gap size between the maximum (minimum) η coverage of the experiment and the nearest detected particle on each side. In order to combine both hemispheres, we define $\tilde{\eta}$ as the minimum of $\eta_{\max}$ and $-\eta_{\min}$. The size of the pseudorapidity gap is then $\Delta\eta_{\text{gap}}^{4.9} = 4.9 - \tilde{\eta}$, where 4.9 is the largest η value covered by the HF.

Figures 6a and 6b show the $\tilde{\eta}$ distribution in the data and MC simulation with different tunes, for the W decays

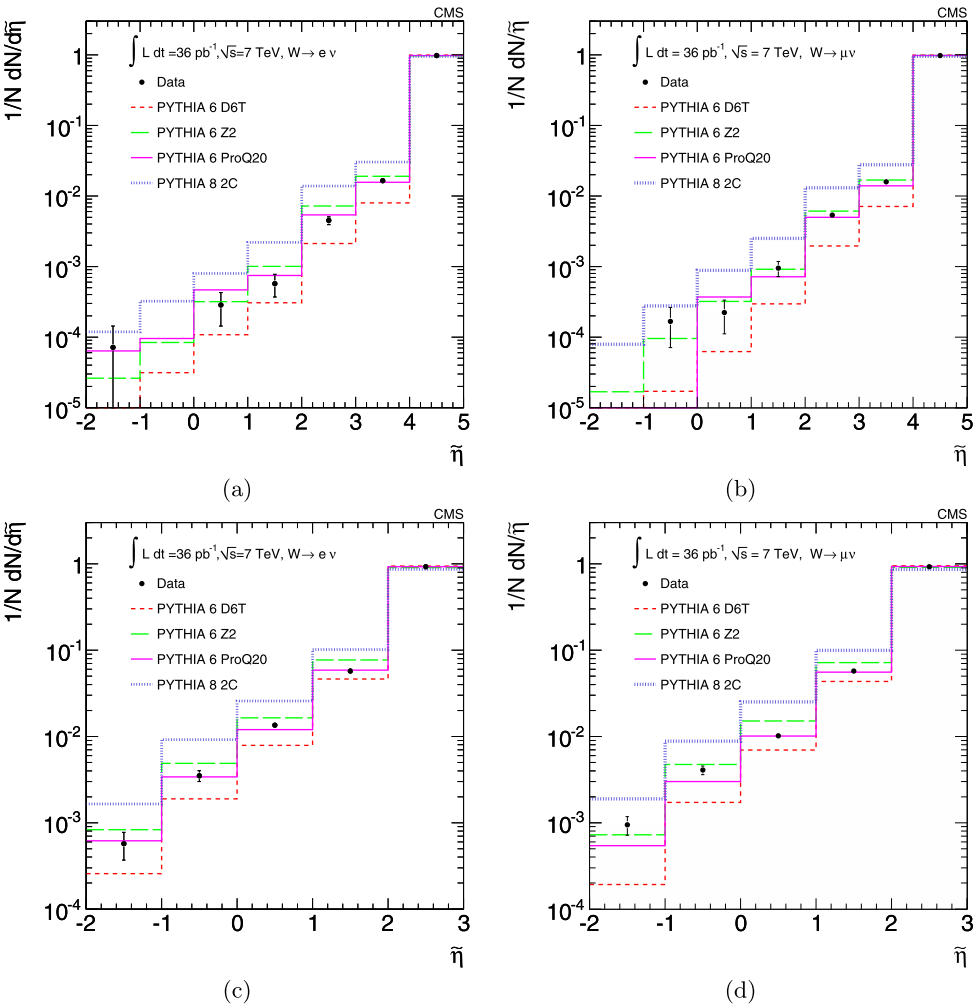

Fig. 6 The $\tilde{\eta}$ distribution for W events with (**a**) electron and (**b**) muon decays in data and for various MC simulations. The corresponding distributions ignoring the HF calorimeter information are shown in (**c**) and (**d**)

to electrons and muons, respectively. The fraction of events with pseudorapidity gaps decreases rapidly when the gap size increases. A statistically significant excess of events at $\tilde{\eta}$ values smaller than 3 is observed, compared to the predictions of the non-diffractive model implemented in PYTHIA6, tune D6T. However, the fraction of events with very large gaps and without a diffractive component in the PYTHIA6 Z2, Pro-Q20, and PYTHIA8 2C tunes and up to the largest observed gap size is larger than in the data.

The stability of the $\tilde{\eta}$ distribution was tested by allowing a $\pm 10\%$ variation of the particle-flow candidate energy and momentum thresholds in the data. The resulting variations were found to be similar to the statistical uncertainties.

If $\tilde{\eta} < 0$, all the reconstructed particle-flow objects in the event are contained in one hemisphere. Combining the W events with LRG signature in both lepton channels, 4 events with one "empty" detector hemisphere, corresponding to a gap of at least $\Delta\eta^{4.9}_{\text{gap}} = 4.9$ units in pseudorapidity, are observed. In comparison, 0.8, 3.5, and 2.2 such events are expected from the non-diffractive MC simulation based on the PYTHIA6 D6T, Z2, and Pro-Q20 tunes, respectively.

As discussed in Sects. 4 and 5, soft pileup events without a detectable second vertex remain in the sample. However, since these events do not produce significant particle-flow in the central pseudorapidity regions, the effect on events with pseudorapidity gaps in the more central region, $|\eta| < 2.85$, is expected to be small. The number of pseudorapidity gap events in this detector region, when ignoring the information in the HF detectors, should mainly depend on the amount of very low multi-parton activity and thus on the number of low-multiplicity events. The $\tilde{\eta}$ distributions using only particle-flow objects with $|\eta| < 2.85$ and ignoring the information in the HF are shown for W events in Figs. 6c and 6d. Accordingly, the gap size is now defined as $\Delta\eta^{2.85}_{\text{gap}} = 2.85 - \tilde{\eta}$. Again, when compared to the MC simulation with the D6T tune, the data show a large excess of events with $\tilde{\eta}$ below 1, corresponding to a central pseudorapidity gap of $\Delta\eta^{2.85}_{\text{gap}} \geq 1.85$. The fraction of such gap events in the data is reasonably well described by the PYTHIA6 Z2

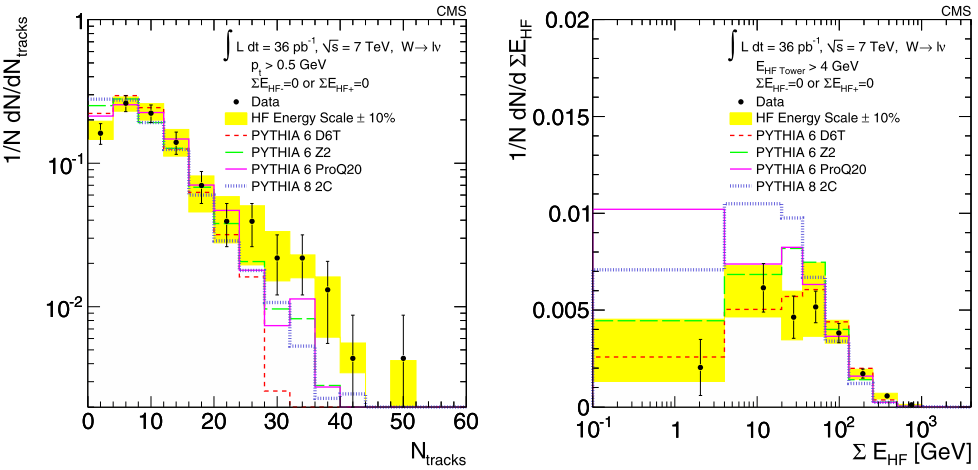

Fig. 7 (**a**) Charged-particle multiplicity and (**b**) HF energy distributions (opposite to the gap) in pp → $W^{\pm}X \to \ell^{\pm}\nu X$ events with a LRG signature, for the data and different MC tunes. The charged-particle multiplicity distribution is obtained for a track p_T threshold of 0.5 GeV

and Pro-Q20 tunes, and much larger fractions are predicted by the PYTHIA8 2C tune.

The limited number of LRG events, as well as the large uncertainties related to the modeling of the underlying event and multi-parton interactions, prevent any conclusions from being drawn on the possible presence of a diffractive W/Z-production component from the observed rate of events with a pseudorapidity gap in the central detector.

6.4 Charged-particle multiplicity and forward energy distributions in LRG events

The charged-particle multiplicity distribution in LRG events, from combining the W events in the electron and muon channels, is shown in Fig. 7a for a minimum track p_T of 0.5 GeV. A slight excess of events with large charged-particle multiplicities is found in the data, compared to the various non diffractive MC tunes. However, overall the track p_T spectrum is well described. The number of LRG events with 20 and more tracks, combining the electron and muon channels, is 33 in the data. Only 13 (19) events with more than 20 tracks are expected from the D6T (Z2) tunes. A similar, but statistically less significant, excess of events with multiplicities larger than predicted by the different tunes is also observed when a track threshold of $p_T > 1.0$ GeV is required.

The POMPYT diffractive model, which does not include multi-parton interactions, predicts even smaller charged-particle multiplicities. However, the observed excess of events with relatively large charged-particle multiplicities in LRG events could be an indication of a diffractive component in the multi-parton interactions, as depicted in Figs. 1c and 1f.

The corresponding distribution for the energy sum in the HF calorimeter opposite to the gap is shown in Fig. 7b. The average total energy of 150 GeV with an r.m.s. of 160 GeV is about a factor of two smaller than the one observed for the inclusive HF energy distribution, and is reasonably well described by the various MC tunes. In the data, we find 2 events with no towers above the energy threshold of 4 GeV in either HF calorimeters, in agreement with the expectation from the D6T tune. This number is slightly lower, but still consistent, with the expectations from the Z2 and the PYTHIA8 2C tunes. The Pro-Q20 tune predicts 8 such events.

6.5 Hemisphere correlations between the gap and the W (Z) boson

Figure 8 shows the distribution of the signed charged lepton pseudorapidity η_ℓ in W events with a LRG signature

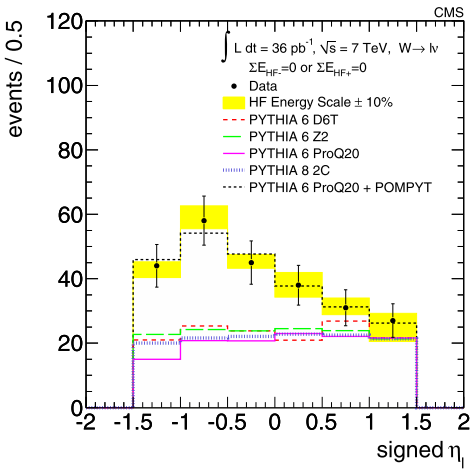

Fig. 8 Signed lepton pseudorapidity distribution in W events with a LRG signature, with the sign defined by the pseudorapidity of the lepton relative to the gap (positive for the lepton and gap in the same hemisphere, negative otherwise). Electron and muon channels are combined. The fit result for the combination of PYTHIA6 (Pro-Q20 tune) and POMPYT predictions is shown as a dotted black line. For the other PYTHIA tunes, only the non-diffractive component is shown

(electron and muon channels combined). The sign is defined to be positive when the gap and the lepton are in the same hemisphere and negative otherwise. The data show that charged leptons from W decays are found more often in the hemisphere opposite to the gap. Combining the electron and muon channels, 147 events are found with the charged lepton in the hemisphere opposite to the gap and 96 events with the lepton in the same hemisphere. Defining an asymmetry as the ratio of the difference between the numbers of LRG events in each hemisphere and the sum, the corresponding asymmetry is $(-21.0 \pm 6.4)\%$. In the case of Z candidates (the rapidity of the Z is used) with a LRG signature, 24 (16) events are in the opposite (same) hemisphere as the gap, resulting in an asymmetry of $(-20 \pm 16)\%$.

In comparison, the various non-diffractive MC tunes predict a symmetric lepton pseudorapidity distribution in LRG events. On the other hand, events generated with the POMPYT generator, based on a diffractive production model, exhibit a strong asymmetry. This can be explained in terms of diffractive PDFs, which peak at smaller x (the parton momentum divided by the proton momentum) than the conventional proton PDFs. The produced W(Z) is thus boosted in the direction of the parton that had the larger x. This is typically the direction of the dissociated proton, i.e., opposite to the gap. The signed lepton pseudorapidity distribution in the data is fit to the predictions from the diffractive POMPYT and the non-diffractive PYTHIA event generators, with the relative fraction of the two as the free parameter. The fit results in a fraction of diffractive events in the LRG sample of $(50.0 \pm 9.3$ (stat.) $\pm$ 5.2 (syst.))%, assuming the model of diffraction implemented in POMPYT and using the PYTHIA6 Pro-Q20 for the simulation of non-diffractive events. The fit results are shown in Fig. 8. The fits using the combination of POMPYT with other tunes give similar results, and only the non-diffractive contribution from the other tunes is shown in Fig. 8. The systematic uncertainty of 5.2% has been determined from the 10% HF energy scale variations and from the fits with the different tunes, using the maximal and minimal fractions obtained from the different fits.

The asymmetry in the signed η_ℓ distribution for non-LRG events is found to decrease when the forward energy deposition increases. For example, for HF energy depositions in the intervals 20–100 GeV, 200–400 GeV, and >500 GeV, the asymmetry is $(-3.5 \pm 1.1)\%$, $(-2.7 \pm 1.0)\%$, and $(0.9 \pm 2.3)\%$. The small residual asymmetry in events with low HF energy depositions is insignificant in comparison to the one in LRG events. However, this could be explained by the presence of a small fraction of diffractively produced W bosons events in which the LRG signature is destroyed by the accompanying multi-parton interaction or by the undetected pileup component. For higher energy depositions in the forward region, the asymmetry vanishes.

7 Conclusions

Central charged-particle multiplicities, forward energy flow, and correlations between them have been studied in W and Z events, identified by the vector–boson decays to electrons and muons, using the 2010 data sample of pp collisions at 7 TeV, corresponding to an integrated luminosity of 36 pb^{-1}.

None of the studied MC tunes provides simultaneously a satisfactory description of the charged-particle multiplicity in the central pseudorapidity region ($|\eta| < 2.5$) and the forward energy flow ($3 < |\eta| < 4.9$). The PYTHIA6 Z2 and PYTHIA8 2C tunes give a reasonable description of the central charged-particle multiplicity, but predict too many events with relatively low-energy depositions in the forward calorimeters. The PYTHIA6 D6T tune predicts too many events with high charged-particle multiplicities, too few events with low-energy depositions, and too many events with very large energy depositions in the forward calorimeters. The Pro-Q20 tune provides the best description of the forward energy distribution and a good description of the charged-particle multiplicity, when a track p_T threshold of 0.5 GeV is applied. However, the charged-particle multiplicity with $p_T > 1.0$ GeV is not well described, though the prediction is closer to the data than that for the D6T tune.

Strong positive correlations between the energy measured in the two forward calorimeters (i.e. at positive and negative rapidities) and the charged-particle multiplicity are observed in the data and in Monte Carlo models. However, the correlations in the various MC tunes are different from those seen in the data.

As far as the LRG events are concerned, the following observations can be made:

- Out of a sample of about 40 000 W and Z events, almost 300 events with a LRG signature are found. According to the POMPYT model of diffractive W production, such events can be interpreted as diffractive. However, while the observed fraction of such events is significantly larger than predicted with the non-diffractive PYTHIA6 D6T tune, it is smaller than expected from the PYTHIA6 Z2, Pro-Q20, and PYTHIA8 2C tunes. Thus, no conclusions can be drawn from the presence of LRG events.
- The central charged-particle multiplicity in these events is somewhat larger than predicted by the various models.
- The HF energy distribution opposite to the gap peaks at much smaller values than in the inclusive events, and is reasonably well described by the MC generators.
- A large asymmetry is observed between the number of events with the charged lepton (from the W decay) in the opposite and with it in the same hemisphere as the pseudorapidity gap. Such an asymmetry is predicted by POMPYT, in contrast to the various non-diffractive PYTHIA MC tunes. When fitting the observed asymmetry in LRG events with an admixture of diffractive (POMPYT)

and non-diffractive (PYTHIA) events, the diffractive component is determined to be $(50.0 \pm 9.3\ (\text{stat.}) \pm 5.2\ (\text{syst.}))\%$, thus providing the first evidence for diffractive W production at the LHC. A comparable, but statistically less significant asymmetry is seen in Z events with large pseudorapidity gaps.

Acknowledgements We wish to congratulate our colleagues in the CERN accelerator departments for the excellent performance of the LHC machine. We would like to thank P. Skands for many explanations and discussions concerning the different underlying event tunes. We would also like to thank the technical and administrative staff at CERN and other CMS institutes, and acknowledge support from: FMSR (Austria); FNRS and FWO (Belgium); CNPq, CAPES, FAPERJ, and FAPESP (Brazil); MES (Bulgaria); CERN; CAS, MoST, and NSFC (China); COLCIENCIAS (Colombia); MSES (Croatia); RPF (Cyprus); Academy of Sciences and NICPB (Estonia); Academy of Finland, ME, and HIP (Finland); CEA and CNRS/IN2P3 (France); BMBF, DFG, and HGF (Germany); GSRT (Greece); OTKA and NKTH (Hungary); DAE and DST (India); IPM (Iran); SFI (Ireland); INFN (Italy); NRF and WCU (Korea); LAS (Lithuania); CINVESTAV, CONACYT, SEP, and UASLP-FAI (Mexico); PAEC (Pakistan); SCSR (Poland); FCT (Portugal); JINR (Armenia, Belarus, Georgia, Ukraine, Uzbekistan); MST and MAE (Russia); MSTDS (Serbia); MICINN and CPAN (Spain); Swiss Funding Agencies (Switzerland); NSC (Taipei); TUBITAK and TAEK (Turkey); STFC (United Kingdom); DOE and NSF (USA). Individuals have received support from the Marie-Curie IEF program (European Union); the Leventis Foundation; the A. P. Sloan Foundation; the Alexander von Humboldt Foundation; and the Associazione per lo Sviluppo Scientifico e Tecnologico del Piemonte (Italy).

References

1. CMS Collaboration, Measurement of the underlying event activity at the LHC with $\sqrt{s} = 7$ TeV and comparison with $\sqrt{s} =$ 0.9 TeV. J. High Energy Phys. **09**, 109 (2011). doi:10.1007/JHEP09(2011)109
2. P. Collins, *An Introduction to Regge Theory and High-Energy Physics* (Cambridge University Press, Cambridge, 1977)
3. UA8 Collaboration, Measurements of single diffraction at $\sqrt{s} =$ 630 GeV: evidence for a non-linear $\alpha(t)$ of the pomeron. Nucl. Phys. B **514**, 3 (1998). doi:10.1016/S0550-3213(97)00813-4
4. ZEUS Collaboration, A QCD analysis of ZEUS diffractive data. Nucl. Phys. B **831**, 1 (2010). arXiv:0911.4119. doi:10.1016/j.nuclphysb.2010.01.014.
5. H1 Collaboration, Dijet cross sections and parton densities in diffractive DIS at HERA. J. High Energy Phys. **0710**, 042 (2007). arXiv:0708.3217. doi:10.1088/1126-6708/2007/10/042.
6. H1 Collaboration, Measurement and QCD analysis of the diffractive deep-inelastic scattering cross-section at HERA. Eur. Phys. J. C **48**, 715 (2006). arXiv:hep-ex/0606004. doi:10.1140/epjc/s10052-006-0035-3
7. CDF Collaboration, Observation of diffractive W boson production at the Tevatron. Phys. Rev. Lett. **78**, 2698 (1997). arXiv:hep-ex/9703010. doi:10.1103/PhysRevLett.78.2698
8. D0 Collaboration, Observation of diffractively produced W and Z bosons in $\bar{p}p$ collisions at $\sqrt{s} = 1800$ GeV. Phys. Lett. B **574**, 169 (2003). arXiv:hep-ex/0308032. doi:10.1016/j.physletb.2003.09.001
9. J.C. Collins, Proof of factorization for diffractive hard scattering. Phys. Rev. D **57**, 3051 (1998). arXiv:hep-ph/9709499. doi:10.1103/PhysRevD.57.3051
10. J.D. Bjorken, Rapidity gaps and jets as a new physics signature in very high-energy hadron hadron collisions. Phys. Rev. D **47**, 101 (1993). doi:10.1103/PhysRevD.47.101
11. A.B. Kaidalov, V.A. Khoze, A.D. Martin et al., Probabilities of rapidity gaps in high-energy interactions. Eur. Phys. J. D **21**, 521 (2001). arXiv:hep-ph/0105145. doi:10.1007/s100520100751
12. CDF Collaboration, Diffractive W and Z production at the fermilab Tevatron. Phys. Rev. D **82**, 112004 (2010). arXiv:1007.5048. doi:10.1103/PhysRevD.82.112004
13. T. Sjostrand, S. Mrenna, P.Z. Skands, PYTHIA 6.4 physics and manual. J. High Energy Phys. **05**, 026 (2006). arXiv:hep-ph/0603175. doi:10.1088/1126-6708/2006/05/026
14. T. Sjostrand, S. Mrenna, P. Skands, A brief introduction to PYTHIA 8.1. Comp. Phys. Com. **178** (2008). arXiv:0710.3820. doi:10.1016/j.cpc.2008.01.036
15. P. Bartalini, L. Fanó (eds.), *Multiple parton interactions at the LHC*. Proceedings, 1st Workshop, DESY-PROC-2009-06, Perugia, Italy, October 27–31, 2008 (2009)
16. R. Field, Studying the underlying event at CDF and the LHC, in *Proceedings of the First International Workshop on Multiple Partonic Interactions at the LHC MPI'08*, ed. by P. Bartalini, L. Fanó. Perugia, Italy, October 27–31, 2008 (2009), pp. 12–31. arXiv:1003.4220
17. A. Buckley et al., Systematic event generator tuning for the LHC. Eur. Phys. J. C **65**, 331 (2010). arXiv:0907.2973. doi:10.1140/epjc/s10052-009-1196-7
18. P.Z. Skands, Tuning Monte Carlo generators: the Perugia tunes. Phys. Rev. D **82**, 074018 (2010). arXiv:1005.3457. doi:10.1103/PhysRevD.82.074018
19. R. Field, Early LHC underlying event data—findings and surprises (2010). arXiv:1010.3558
20. R. Corke, T. Sjöstrand, Interleaved parton showers and tuning prospects. J. High Energy Phys. **03**, 032 (2011). arXiv:1011.1759. doi:10.1007/JHEP03(2011)032
21. P.M. Nadolsky et al., Implications of CTEQ global analysis for collider observables. Phys. Rev. D **78**, 013004 (2008). arXiv:0802.0007. doi:10.1103/PhysRevD.78.013004
22. P. Bruni, G. Ingelman, Diffractive W and Z production at $p\bar{p}$ colliders and the pomeron parton content. Phys. Lett. B **311**, 317 (1993). doi:10.1016/0370-2693(93)90576-4
23. P. Bruni, G. Ingelman, Diffractive hard scattering at ep and $p\bar{p}$ colliders, in *Proceedings of the International Europhysics Conference on High Energy Physics*, Marseille, France, 22–28 Jul 1993 (1994), p. 595
24. H1 Collaboration, Dijet cross sections and parton densities in diffractive DIS at HERA. J. High Energy Phys. **10**, 042 (2007). arXiv:0708.3217. doi:10.1088/1126-6708/2007/10/042
25. CMS Collaboration, The CMS experiment at the CERN LHC. J. Instrum. **0803**, S08004 (2008). doi:10.1088/1748-0221/3/08/S08004
26. CMS Collaboration, Measurements of inclusive W and Z cross sections in pp collisions at $\sqrt{s} = 7$ TeV. J. High Energy Phys. **01**, 080 (2011). arXiv:1012.2466. doi:10.1007/JHEP01(2011)080
27. CMS Collaboration, Commissioning of the particle-flow reconstruction in minimum-bias and jet events from pp collisions at 7 TeV, CMS Physics Analysis Summary CMS-PAS-PFT-10-002 (2010)
28. M. Cacciari, G.P. Salam, G. Soyez, The anti-k_t jet clustering algorithm. J. High Energy Phys. **04**, 063 (2008). doi:10.1088/1126-6708/2008/04/063
29. ATLAS Collaboration, Measurement of the inelastic proton–proton cross-section at $\sqrt{s} = 7$ TeV with the ATLAS detector (2011). arXiv:1104.0326

30. TOTEM Collaboration, Proton–proton elastic scattering at the LHC energy of $\sqrt{s} = 7$ TeV. Europhys. Lett. **95**, 41001 (2011). doi:10.1209/0295-5075/95/41001

31. CMS Collaboration, CMS tracking performance results from early LHC operation. Eur. Phys. J. C **70**, 1165 (2010). arXiv:1007.1988. doi:10.1140/epjc/s10052-010-1491-3

The CMS Collaboration

Yerevan Physics Institute, Yerevan, Armenia
S. Chatrchyan, V. Khachatryan, A.M. Sirunyan, A. Tumasyan

Institut für Hochenergiephysik der OeAW, Wien, Austria
W. Adam, T. Bergauer, M. Dragicevic, J. Erö, C. Fabjan, M. Friedl, R. Frühwirth, V.M. Ghete, J. Hammer[1], S. Hänsel, M. Hoch, N. Hörmann, J. Hrubec, M. Jeitler, W. Kiesenhofer, M. Krammer, D. Liko, I. Mikulec, M. Pernicka, B. Rahbaran, H. Rohringer, R. Schöfbeck, J. Strauss, A. Taurok, F. Teischinger, C. Trauner, P. Wagner, W. Waltenberger, G. Walzel, E. Widl, C.-E. Wulz

National Centre for Particle and High Energy Physics, Minsk, Belarus
V. Mossolov, N. Shumeiko, J. Suarez Gonzalez

Universiteit Antwerpen, Antwerpen, Belgium
S. Bansal, L. Benucci, E.A. De Wolf, X. Janssen, T. Maes, L. Mucibello, S. Ochesanu, B. Roland, R. Rougny, M. Selvaggi, H. Van Haevermaet, P. Van Mechelen, N. Van Remortel

Vrije Universiteit Brussel, Brussel, Belgium
F. Blekman, S. Blyweert, J. D'Hondt, O. Devroede, R. Gonzalez Suarez, A. Kalogeropoulos, M. Maes, W. Van Doninck, P. Van Mulders, G.P. Van Onsem, I. Villella

Université Libre de Bruxelles, Bruxelles, Belgium
O. Charaf, B. Clerbaux, G. De Lentdecker, V. Dero, A.P.R. Gay, G.H. Hammad, T. Hreus, P.E. Marage, A. Raval, L. Thomas, G. Vander Marcken, C. Vander Velde, P. Vanlaer

Ghent University, Ghent, Belgium
V. Adler, A. Cimmino, S. Costantini, M. Grunewald, B. Klein, J. Lellouch, A. Marinov, J. Mccartin, D. Ryckbosch, F. Thyssen, M. Tytgat, L. Vanelderen, P. Verwilligen, S. Walsh, N. Zaganidis

Université Catholique de Louvain, Louvain-la-Neuve, Belgium
S. Basegmez, G. Bruno, J. Caudron, L. Ceard, E. Cortina Gil, J. De Favereau De Jeneret, C. Delaere, D. Favart, A. Giammanco, G. Grégoire, J. Hollar, V. Lemaitre, J. Liao, O. Militaru, C. Nuttens, S. Ovyn, D. Pagano, A. Pin, K. Piotrzkowski, N. Schul

Université de Mons, Mons, Belgium
N. Beliy, T. Caebergs, E. Daubie

Centro Brasileiro de Pesquisas Fisicas, Rio de Janeiro, Brazil
G.A. Alves, L. Brito, D. De Jesus Damiao, M.E. Pol, M.H.G. Souza

Universidade do Estado do Rio de Janeiro, Rio de Janeiro, Brazil
W.L. Aldá Júnior, W. Carvalho, E.M. Da Costa, C. De Oliveira Martins, S. Fonseca De Souza, D. Matos Figueiredo, L. Mundim, H. Nogima, V. Oguri, W.L. Prado Da Silva, A. Santoro, S.M. Silva Do Amaral, A. Sznajder

Instituto de Fisica Teorica, Universidade Estadual Paulista, Sao Paulo, Brazil
T.S. Anjos[2], C.A. Bernardes[2], F.A. Dias[3], T.R. Fernandez Perez Tomei, E.M. Gregores[2], C. Lagana, F. Marinho, P.G. Mercadante[2], S.F. Novaes, S.S. Padula

Institute for Nuclear Research and Nuclear Energy, Sofia, Bulgaria
N. Darmenov[1], V. Genchev[1], P. Iaydjiev[1], S. Piperov, M. Rodozov, S. Stoykova, G. Sultanov, V. Tcholakov, R. Trayanov

University of Sofia, Sofia, Bulgaria
A. Dimitrov, R. Hadjiiska, A. Karadzhinova, V. Kozhuharov, L. Litov, M. Mateev, B. Pavlov, P. Petkov

Institute of High Energy Physics, Beijing, China
J.G. Bian, G.M. Chen, H.S. Chen, C.H. Jiang, D. Liang, S. Liang, X. Meng, J. Tao, J. Wang, J. Wang, X. Wang, Z. Wang, H. Xiao, M. Xu, J. Zang, Z. Zhang

State Key Lab. of Nucl. Phys. and Tech., Peking University, Beijing, China
Y. Ban, S. Guo, Y. Guo, W. Li, Y. Mao, S.J. Qian, H. Teng, B. Zhu, W. Zou

Universidad de Los Andes, Bogota, Colombia
A. Cabrera, B. Gomez Moreno, A.A. Ocampo Rios, A.F. Osorio Oliveros, J.C. Sanabria

Technical University of Split, Split, Croatia
N. Godinovic, D. Lelas, K. Lelas, R. Plestina[4], D. Polic, I. Puljak

University of Split, Split, Croatia
Z. Antunovic, M. Dzelalija

Institute Rudjer Boskovic, Zagreb, Croatia
V. Brigljevic, S. Duric, K. Kadija, J. Luetic, S. Morovic

University of Cyprus, Nicosia, Cyprus
A. Attikis, M. Galanti, J. Mousa, C. Nicolaou, F. Ptochos, P.A. Razis

Charles University, Prague, Czech Republic
M. Finger, M. Finger Jr.

Academy of Scientific Research and Technology of the Arab Republic of Egypt, Egyptian Network of High Energy Physics, Cairo, Egypt
Y. Assran[5], A. Ellithi Kamel[6], S. Khalil[7], M.A. Mahmoud[8], A. Radi[9]

National Institute of Chemical Physics and Biophysics, Tallinn, Estonia
A. Hektor, M. Kadastik, M. Müntel, M. Raidal, L. Rebane, A. Tiko

Department of Physics, University of Helsinki, Helsinki, Finland
V. Azzolini, P. Eerola, G. Fedi

Helsinki Institute of Physics, Helsinki, Finland
S. Czellar, J. Härkönen, A. Heikkinen, V. Karimäki, R. Kinnunen, M.J. Kortelainen, T. Lampén, K. Lassila-Perini, S. Lehti, T. Lindén, P. Luukka, T. Mäenpää, E. Tuominen, J. Tuominiemi, E. Tuovinen, D. Ungaro, L. Wendland

Lappeenranta University of Technology, Lappeenranta, Finland
K. Banzuzi, A. Karjalainen, A. Korpela, T. Tuuva

Laboratoire d'Annecy-le-Vieux de Physique des Particules, IN2P3-CNRS, Annecy-le-Vieux, France
D. Sillou

DSM/IRFU, CEA/Saclay, Gif-sur-Yvette, France
M. Besancon, S. Choudhury, M. Dejardin, D. Denegri, B. Fabbro, J.L. Faure, F. Ferri, S. Ganjour, F.X. Gentit, A. Givernaud, P. Gras, G. Hamel de Monchenault, P. Jarry, E. Locci, J. Malcles, M. Marionneau, L. Millischer, J. Rander, A. Rosowsky, I. Shreyber, M. Titov, P. Verrecchia

Laboratoire Leprince-Ringuet, Ecole Polytechnique, IN2P3-CNRS, Palaiseau, France
S. Baffioni, F. Beaudette, L. Benhabib, L. Bianchini, M. Bluj[10], C. Broutin, P. Busson, C. Charlot, T. Dahms, L. Dobrzynski, S. Elgammal, R. Granier de Cassagnac, M. Haguenauer, P. Miné, C. Mironov, C. Ochando, P. Paganini, D. Sabes, R. Salerno, Y. Sirois, C. Thiebaux, B. Wyslouch[11], A. Zabi

Université de Strasbourg, Université de Haute Alsace Mulhouse, CNRS/IN2P3, Institut Pluridisciplinaire Hubert Curien, Strasbourg, France
J.-L. Agram[12], J. Andrea, D. Bloch, D. Bodin, J.-M. Brom, M. Cardaci, E.C. Chabert, C. Collard, E. Conte[12], F. Drouhin[12], C. Ferro, J.-C. Fontaine[12], D. Gelé, U. Goerlach, S. Greder, P. Juillot, M. Karim[12], A.-C. Le Bihan, Y. Mikami, P. Van Hove

Centre de Calcul de l'Institut National de Physique Nucleaire et de Physique des Particules (IN2P3), Villeurbanne, France
F. Fassi, D. Mercier

Université de Lyon, Université Claude Bernard Lyon 1, CNRS-IN2P3, Institut de Physique Nucléaire de Lyon, Villeurbanne, France
C. Baty, S. Beauceron, N. Beaupere, M. Bedjidian, O. Bondu, G. Boudoul, D. Boumediene, H. Brun, J. Chasserat, R. Chierici, D. Contardo, P. Depasse, H. El Mamouni, J. Fay, S. Gascon, B. Ille, T. Kurca, T. Le Grand, M. Lethuillier, L. Mirabito, S. Perries, V. Sordini, S. Tosi, Y. Tschudi, P. Verdier

Institute of High Energy Physics and Informatization, Tbilisi State University, Tbilisi, Georgia
D. Lomidze

RWTH Aachen University, I. Physikalisches Institut, Aachen, Germany
G. Anagnostou, S. Beranek, M. Edelhoff, L. Feld, N. Heracleous, O. Hindrichs, R. Jussen, K. Klein, J. Merz, N. Mohr, A. Ostapchuk, A. Perieanu, F. Raupach, J. Sammet, S. Schael, D. Sprenger, H. Weber, M. Weber, B. Wittmer

RWTH Aachen University, III. Physikalisches Institut A, Aachen, Germany
M. Ata, E. Dietz-Laursonn, M. Erdmann, T. Hebbeker, C. Heidemann, A. Hinzmann, K. Hoepfner, T. Klimkovich, D. Klingebiel, P. Kreuzer, D. Lanske[†], J. Lingemann, C. Magass, M. Merschmeyer, A. Meyer, P. Papacz, H. Pieta, H. Reithler, S.A. Schmitz, L. Sonnenschein, J. Steggemann, D. Teyssier

RWTH Aachen University, III. Physikalisches Institut B, Aachen, Germany
M. Bontenackels, M. Davids, M. Duda, G. Flügge, H. Geenen, M. Giffels, W. Haj Ahmad, D. Heydhausen, F. Hoehle, B. Kargoll, T. Kress, Y. Kuessel, A. Linn, A. Nowack, L. Perchalla, O. Pooth, J. Rennefeld, P. Sauerland, A. Stahl, D. Tornier, M.H. Zoeller

Deutsches Elektronen-Synchrotron, Hamburg, Germany
M. Aldaya Martin, W. Behrenhoff, U. Behrens, M. Bergholz[13], A. Bethani, K. Borras, A. Cakir, A. Campbell, E. Castro, D. Dammann, G. Eckerlin, D. Eckstein, A. Flossdorf, G. Flucke, A. Geiser, J. Hauk, H. Jung[1], M. Kasemann, P. Katsas, C. Kleinwort, H. Kluge, A. Knutsson, M. Krämer, D. Krücker, E. Kuznetsova, W. Lange, W. Lohmann[13], R. Mankel, M. Marienfeld, I.-A. Melzer-Pellmann, A.B. Meyer, J. Mnich, A. Mussgiller, J. Olzem, A. Petrukhin, D. Pitzl, A. Raspereza, M. Rosin, R. Schmidt[13], T. Schoerner-Sadenius, N. Sen, A. Spiridonov, M. Stein, J. Tomaszewska, R. Walsh, C. Wissing

University of Hamburg, Hamburg, Germany
C. Autermann, V. Blobel, S. Bobrovskyi, J. Draeger, H. Enderle, U. Gebbert, M. Görner, T. Hermanns, K. Kaschube, G. Kaussen, H. Kirschenmann, R. Klanner, J. Lange, B. Mura, S. Naumann-Emme, F. Nowak, N. Pietsch, C. Sander, H. Schettler, P. Schleper, E. Schlieckau, M. Schröder, T. Schum, H. Stadie, G. Steinbrück, J. Thomsen

Institut für Experimentelle Kernphysik, Karlsruhe, Germany
C. Barth, J. Bauer, J. Berger, V. Buege, T. Chwalek, W. De Boer, A. Dierlamm, G. Dirkes, M. Feindt, J. Gruschke, C. Hackstein, F. Hartmann, M. Heinrich, H. Held, K.H. Hoffmann, S. Honc, I. Katkov[14], J.R. Komaragiri, T. Kuhr, D. Martschei, S. Mueller, Th. Müller, M. Niegel, O. Oberst, A. Oehler, J. Ott, T. Peiffer, G. Quast, K. Rabbertz, F. Ratnikov, N. Ratnikova, M. Renz, C. Saout, A. Scheurer, P. Schieferdecker, F.-P. Schilling, G. Schott, H.J. Simonis, F.M. Stober, D. Troendle, J. Wagner-Kuhr, T. Weiler, M. Zeise, V. Zhukov[14], E.B. Ziebarth

Institute of Nuclear Physics "Demokritos", Aghia Paraskevi, Greece
G. Daskalakis, T. Geralis, S. Kesisoglou, A. Kyriakis, D. Loukas, I. Manolakos, A. Markou, C. Markou, C. Mavrommatis, E. Ntomari, E. Petrakou

University of Athens, Athens, Greece
L. Gouskos, T.J. Mertzimekis, A. Panagiotou, N. Saoulidou, E. Stiliaris

University of Ioánnina, Ioánnina, Greece
I. Evangelou, C. Foudas, P. Kokkas, N. Manthos, I. Papadopoulos, V. Patras, F.A. Triantis

KFKI Research Institute for Particle and Nuclear Physics, Budapest, Hungary
A. Aranyi, G. Bencze, L. Boldizsar, C. Hajdu[1], P. Hidas, D. Horvath[15], A. Kapusi, K. Krajczar[16], F. Sikler[1], G.I. Veres[16], G. Vesztergombi[16]

Institute of Nuclear Research ATOMKI, Debrecen, Hungary
N. Beni, J. Molnar, J. Palinkas, Z. Szillasi, V. Veszpremi

University of Debrecen, Debrecen, Hungary
P. Raics, Z.L. Trocsanyi, B. Ujvari

Panjab University, Chandigarh, India
S.B. Beri, V. Bhatnagar, N. Dhingra, R. Gupta, M. Jindal, M. Kaur, J.M. Kohli, M.Z. Mehta, N. Nishu, L.K. Saini, A. Sharma, A.P. Singh, J. Singh, S.P. Singh

University of Delhi, Delhi, India
S. Ahuja, B.C. Choudhary, P. Gupta, A. Kumar, A. Kumar, S. Malhotra, M. Naimuddin, K. Ranjan, R.K. Shivpuri

Saha Institute of Nuclear Physics, Kolkata, India
S. Banerjee, S. Bhattacharya, S. Dutta, B. Gomber, S. Jain, S. Jain, R. Khurana, S. Sarkar

Bhabha Atomic Research Centre, Mumbai, India
R.K. Choudhury, D. Dutta, S. Kailas, V. Kumar, P. Mehta, A.K. Mohanty[1], L.M. Pant, P. Shukla

Tata Institute of Fundamental Research—EHEP, Mumbai, India
T. Aziz, M. Guchait[17], A. Gurtu, M. Maity[18], D. Majumder, G. Majumder, K. Mazumdar, G.B. Mohanty, A. Saha, K. Sudhakar, N. Wickramage

Tata Institute of Fundamental Research—HECR, Mumbai, India
S. Banerjee, S. Dugad, N.K. Mondal

Institute for Research and Fundamental Sciences (IPM), Tehran, Iran
H. Arfaei, H. Bakhshiansohi[19], S.M. Etesami[20], A. Fahim[19], M. Hashemi, H. Hesari, A. Jafari[19], M. Khakzad, A. Mohammadi[21], M. Mohammadi Najafabadi, S. Paktinat Mehdiabadi, B. Safarzadeh, M. Zeinali[20]

INFN Sezione di Bari[a], Università di Bari[b], Politecnico di Bari[c], Bari, Italy
M. Abbrescia[a,b], L. Barbone[a,b], C. Calabria[a,b], A. Colaleo[a], D. Creanza[a,c], N. De Filippis[a,c,1], M. De Palma[a,b], L. Fiore[a], G. Iaselli[a,c], L. Lusito[a,b], G. Maggi[a,c], M. Maggi[a], N. Manna[a,b], B. Marangelli[a,b], S. My[a,c], S. Nuzzo[a,b], N. Pacifico[a,b], G.A. Pierro[a], A. Pompili[a,b], G. Pugliese[a,c], F. Romano[a,c], G. Roselli[a,b], G. Selvaggi[a,b], L. Silvestris[a], R. Trentadue[a], S. Tupputi[a,b], G. Zito[a]

INFN Sezione di Bologna[a], Università di Bologna[b], Bologna, Italy
G. Abbiendi[a], A.C. Benvenuti[a], D. Bonacorsi[a], S. Braibant-Giacomelli[a,b], L. Brigliadori[a], P. Capiluppi[a,b], A. Castro[a,b], F.R. Cavallo[a], M. Cuffiani[a,b], G.M. Dallavalle[a], F. Fabbri[a], A. Fanfani[a,b], D. Fasanella[a], P. Giacomelli[a], M. Giunta[a], C. Grandi[a], S. Marcellini[a], G. Masetti[b], M. Meneghelli[a,b], A. Montanari[a], F.L. Navarria[a,b], F. Odorici[a], A. Perrotta[a], F. Primavera[a], A.M. Rossi[a,b], T. Rovelli[a,b], G. Siroli[a,b], R. Travaglini[a,b]

INFN Sezione di Catania[a], Università di Catania[b], Catania, Italy
S. Albergo[a,b], G. Cappello[a,b], M. Chiorboli[a,b,1], S. Costa[a,b], R. Potenza[a,b], A. Tricomi[a,b], C. Tuve[a,b]

INFN Sezione di Firenze[a], Università di Firenze[b], Firenze, Italy
G. Barbagli[a], V. Ciulli[a,b], C. Civinini[a], R. D'Alessandro[a,b], E. Focardi[a,b], S. Frosali[a,b], E. Gallo[a], S. Gonzi[a,b], P. Lenzi[a,b], M. Meschini[a], S. Paoletti[a], G. Sguazzoni[a], A. Tropiano[a,1]

INFN Laboratori Nazionali di Frascati, Frascati, Italy
L. Benussi, S. Bianco, S. Colafranceschi[22], F. Fabbri, D. Piccolo

INFN Sezione di Genova, Genova, Italy
P. Fabbricatore, R. Musenich

INFN Sezione di Milano-Bicocca[a], Università di Milano-Bicocca[b], Milano, Italy
A. Benaglia[a,b], F. De Guio[a,b,1], L. Di Matteo[a,b], S. Gennai[a,1], A. Ghezzi[a,b], S. Malvezzi[a], A. Martelli[a,b], A. Massironi[a,b], D. Menasce[a], L. Moroni[a], M. Paganoni[a,b], D. Pedrini[a], S. Ragazzi[a,b], N. Redaelli[a], S. Sala[a], T. Tabarelli de Fatis[a,b]

INFN Sezione di Napoli[a], Università di Napoli "Federico II"[b], Napoli, Italy
S. Buontempo[a], C.A. Carrillo Montoya[a,1], N. Cavallo[a,23], A. De Cosa[a,b], F. Fabozzi[a,23], A.O.M. Iorio[a,1], L. Lista[a], M. Merola[a,b], P. Paolucci[a]

INFN Sezione di Padova[a], Università di Padova[b], Università di Trento (Trento)[c], Padova, Italy
P. Azzi[a], N. Bacchetta[a], P. Bellan[a,b], D. Bisello[a,b], A. Branca[a], R. Carlin[a,b], P. Checchia[a], T. Dorigo[a], U. Dosselli[a], F. Fanzago[a], F. Gasparini[a,b], U. Gasparini[a,b], A. Gozzelino[a], S. Lacaprara[a,24], I. Lazzizzera[a,c], M. Margoni[a,b], M. Mazzucato[a], A.T. Meneguzzo[a,b], M. Nespolo[a,1], L. Perrozzi[a,1], N. Pozzobon[a,b], P. Ronchese[a,b], F. Simonetto[a,b], E. Torassa[a], M. Tosi[a,b], S. Vanini[a,b], P. Zotto[a,b], G. Zumerle[a,b]

INFN Sezione di Pavia[a], Università di Pavia[b], Pavia, Italy
P. Baesso[a,b], U. Berzano[a], S.P. Ratti[a,b], C. Riccardi[a,b], P. Torre[a,b], P. Vitulo[a,b], C. Viviani[a,b]

INFN Sezione di Perugia[a], Università di Perugia[b], Perugia, Italy
M. Biasini[a,b], G.M. Bilei[a], B. Caponeri[a,b], L. Fanò[a,b], P. Lariccia[a,b], A. Lucaroni[a,b,1], G. Mantovani[a,b], M. Menichelli[a], A. Nappi[a,b], F. Romeo[a,b], A. Santocchia[a,b], S. Taroni[a,b,1], M. Valdata[a,b]

INFN Sezione di Pisa[a], Università di Pisa[b], Scuola Normale Superiore di Pisa[c], Pisa, Italy
P. Azzurri[a,c], G. Bagliesi[a], J. Bernardini[a,b], T. Boccali[a], G. Broccolo[a,c], R. Castaldi[a], R.T. D'Agnolo[a,c], R. Dell'Orso[a], F. Fiori[a,b], L. Foà[a,c], A. Giassi[a], A. Kraan[a], F. Ligabue[a,c], T. Lomtadze[a], L. Martini[a,25], A. Messineo[a,b], F. Palla[a], F. Palmonari[a], G. Segneri[a], A.T. Serban[a], P. Spagnolo[a], R. Tenchini[a], G. Tonelli[a,b,1], A. Venturi[a,1], P.G. Verdini[a]

INFN Sezione di Roma[a], Università di Roma "La Sapienza"[b], Roma, Italy
L. Barone[a,b], F. Cavallari[a], D. Del Re[a,b], E. Di Marco[a,b], M. Diemoz[a], D. Franci[a,b], M. Grassi[a,1], E. Longo[a,b], P. Meridiani[a], S. Nourbakhsh[a], G. Organtini[a,b], F. Pandolfi[a,b,1], R. Paramatti[a], S. Rahatlou[a,b], C. Rovelli[a,1], M. Sigamani[a]

INFN Sezione di Torino[a], Università di Torino[b], Università del Piemonte Orientale (Novara)[c], Torino, Italy
N. Amapane[a,b], R. Arcidiacono[a,c], S. Argiro[a,b], M. Arneodo[a,c], C. Biino[a], C. Botta[a,b,1], N. Cartiglia[a], R. Castello[a,b], M. Costa[a,b], N. Demaria[a], A. Graziano[a,b,1], C. Mariotti[a], M. Marone[a,b], S. Maselli[a], E. Migliore[a,b], G. Mila[a,b], V. Monaco[a,b], M. Musich[a], M.M. Obertino[a,c], N. Pastrone[a], M. Pelliccioni[a,b], A. Potenza[a,b], A. Romero[a,b], M. Ruspa[a,c], R. Sacchi[a,b], V. Sola[a,b], A. Solano[a,b], A. Staiano[a], A. Vilela Pereira[a]

INFN Sezione di Trieste[a], Università di Trieste[b], Trieste, Italy
S. Belforte[a], F. Cossutti[a], G. Della Ricca[a,b], B. Gobbo[a], D. Montanino[a,b], A. Penzo[a]

Kangwon National University, Chunchon, Korea
S.G. Heo, S.K. Nam

Kyungpook National University, Daegu, Korea
S. Chang, J. Chung, D.H. Kim, G.N. Kim, J.E. Kim, D.J. Kong, H. Park, S.R. Ro, D.C. Son, T. Son

Institute for Universe and Elementary Particles, Chonnam National University, Kwangju, Korea
J.Y. Kim, Z.J. Kim, S. Song

Korea University, Seoul, Korea
S. Choi, B. Hong, M. Jo, H. Kim, J.H. Kim, T.J. Kim, K.S. Lee, D.H. Moon, S.K. Park, K.S. Sim

University of Seoul, Seoul, Korea
M. Choi, S. Kang, H. Kim, C. Park, I.C. Park, S. Park, G. Ryu

Sungkyunkwan University, Suwon, Korea
Y. Choi, Y.K. Choi, J. Goh, M.S. Kim, B. Lee, J. Lee, S. Lee, H. Seo, I. Yu

Vilnius University, Vilnius, Lithuania
M.J. Bilinskas, I. Grigelionis, M. Janulis, D. Martisiute, P. Petrov, M. Polujanskas, T. Sabonis

Centro de Investigacion y de Estudios Avanzados del IPN, Mexico City, Mexico
H. Castilla-Valdez, E. De La Cruz-Burelo, I. Heredia-de La Cruz, R. Lopez-Fernandez, R. Magaña Villalba, A. Sánchez-Hernández, L.M. Villasenor-Cendejas

Universidad Iberoamericana, Mexico City, Mexico
S. Carrillo Moreno, F. Vazquez Valencia

Benemerita Universidad Autonoma de Puebla, Puebla, Mexico
H.A. Salazar Ibarguen

Universidad Autónoma de San Luis Potosí, San Luis Potosí, Mexico
E. Casimiro Linares, A. Morelos Pineda, M.A. Reyes-Santos

University of Auckland, Auckland, New Zealand
D. Krofcheck, J. Tam

University of Canterbury, Christchurch, New Zealand
P.H. Butler, R. Doesburg, H. Silverwood

National Centre for Physics, Quaid-I-Azam University, Islamabad, Pakistan
M. Ahmad, I. Ahmed, M.H. Ansari, M.I. Asghar, H.R. Hoorani, S. Khalid, W.A. Khan, T. Khurshid, S. Qazi, M.A. Shah, M. Shoaib

Institute of Experimental Physics, Faculty of Physics, University of Warsaw, Warsaw, Poland
G. Brona, M. Cwiok, W. Dominik, K. Doroba, A. Kalinowski, M. Konecki, J. Krolikowski

Soltan Institute for Nuclear Studies, Warsaw, Poland
T. Frueboes, R. Gokieli, M. Górski, M. Kazana, K. Nawrocki, K. Romanowska-Rybinska, M. Szleper, G. Wrochna, P. Zalewski

Laboratório de Instrumentação e Física Experimental de Partículas, Lisboa, Portugal
N. Almeida, P. Bargassa, A. David, P. Faccioli, P.G. Ferreira Parracho, M. Gallinaro[1], P. Musella, A. Nayak, J. Pela[1], P.Q. Ribeiro, J. Seixas, J. Varela

Joint Institute for Nuclear Research, Dubna, Russia
S. Afanasiev, I. Belotelov, P. Bunin, I. Golutvin, A. Kamenev, V. Karjavin, G. Kozlov, A. Lanev, P. Moisenz, V. Palichik, V. Perelygin, S. Shmatov, V. Smirnov, A. Volodko, A. Zarubin

Petersburg Nuclear Physics Institute, Gatchina (St Petersburg), Russia
V. Golovtsov, Y. Ivanov, V. Kim, P. Levchenko, V. Murzin, V. Oreshkin, I. Smirnov, V. Sulimov, L. Uvarov, S. Vavilov, A. Vorobyev, An. Vorobyev

Institute for Nuclear Research, Moscow, Russia
Yu. Andreev, A. Dermenev, S. Gninenko, N. Golubev, M. Kirsanov, N. Krasnikov, V. Matveev, A. Pashenkov, A. Toropin, S. Troitsky

Institute for Theoretical and Experimental Physics, Moscow, Russia
V. Epshteyn, V. Gavrilov, V. Kaftanov†, M. Kossov[1], A. Krokhotin, N. Lychkovskaya, V. Popov, G. Safronov, S. Semenov, V. Stolin, E. Vlasov, A. Zhokin

Moscow State University, Moscow, Russia
A. Belyaev, E. Boos, M. Dubinin[3], L. Dudko, A. Ershov, A. Gribushin, O. Kodolova, I. Lokhtin, A. Markina, S. Obraztsov, M. Perfilov, S. Petrushanko, L. Sarycheva, V. Savrin, A. Snigirev

P.N. Lebedev Physical Institute, Moscow, Russia
V. Andreev, M. Azarkin, I. Dremin, M. Kirakosyan, A. Leonidov, G. Mesyats, S.V. Rusakov, A. Vinogradov

State Research Center of Russian Federation, Institute for High Energy Physics, Protvino, Russia
I. Azhgirey, I. Bayshev, S. Bitioukov, V. Grishin[1], V. Kachanov, D. Konstantinov, A. Korablev, V. Krychkine, V. Petrov, R. Ryutin, A. Sobol, L. Tourtchanovitch, S. Troshin, N. Tyurin, A. Uzunian, A. Volkov

Faculty of Physics and Vinca Institute of Nuclear Sciences, University of Belgrade, Belgrade, Serbia
P. Adzic[26], M. Djordjevic, D. Krpic[26], J. Milosevic

Centro de Investigaciones Energéticas Medioambientales y Tecnológicas (CIEMAT), Madrid, Spain
M. Aguilar-Benitez, J. Alcaraz Maestre, P. Arce, C. Battilana, E. Calvo, M. Cepeda, M. Cerrada, M. Chamizo Llatas, N. Colino, B. De La Cruz, A. Delgado Peris, C. Diez Pardos, D. Domínguez Vázquez, C. Fernandez Bedoya, J.P. Fernández Ramos, A. Ferrando, J. Flix, M.C. Fouz, P. Garcia-Abia, O. Gonzalez Lopez, S. Goy Lopez, J.M. Hernandez, M.I. Josa, G. Merino, J. Puerta Pelayo, I. Redondo, L. Romero, J. Santaolalla, M.S. Soares, C. Willmott

Universidad Autónoma de Madrid, Madrid, Spain
C. Albajar, G. Codispoti, J.F. de Trocóniz

Universidad de Oviedo, Oviedo, Spain
J. Cuevas, J. Fernandez Menendez, S. Folgueras, I. Gonzalez Caballero, L. Lloret Iglesias, J.M. Vizan Garcia

Instituto de Física de Cantabria (IFCA), CSIC-Universidad de Cantabria, Santander, Spain
J.A. Brochero Cifuentes, I.J. Cabrillo, A. Calderon, S.H. Chuang, J. Duarte Campderros, M. Felcini[27], M. Fernandez, G. Gomez, J. Gonzalez Sanchez, C. Jorda, P. Lobelle Pardo, A. Lopez Virto, J. Marco, R. Marco, C. Martinez Rivero, F. Matorras, F.J. Munoz Sanchez, J. Piedra Gomez[28], T. Rodrigo, A.Y. Rodríguez-Marrero, A. Ruiz-Jimeno, L. Scodellaro, M. Sobron Sanudo, I. Vila, R. Vilar Cortabitarte

CERN, European Organization for Nuclear Research, Geneva, Switzerland
D. Abbaneo, E. Auffray, G. Auzinger, P. Baillon, A.H. Ball, D. Barney, A.J. Bell[29], D. Benedetti, C. Bernet[4], W. Bialas, P. Bloch, A. Bocci, S. Bolognesi, M. Bona, H. Breuker, K. Bunkowski, T. Camporesi, G. Cerminara, T. Christiansen, J.A. Coarasa Perez, B. Curé, D. D'Enterria, A. De Roeck, S. Di Guida, N. Dupont-Sagorin, A. Elliott-Peisert, B. Frisch, W. Funk, A. Gaddi, G. Georgiou, H. Gerwig, D. Gigi, K. Gill, D. Giordano, F. Glege, R. Gomez-Reino Garrido, M. Gouzevitch, P. Govoni, S. Gowdy, L. Guiducci, M. Hansen, C. Hartl, J. Harvey, J. Hegeman, B. Hegner, H.F. Hoffmann, A. Honma, V. Innocente, P. Janot, K. Kaadze, E. Karavakis, P. Lecoq, C. Lourenço, T. Mäki, M. Malberti, L. Malgeri, M. Mannelli, L. Masetti, A. Maurisset, F. Meijers, S. Mersi, E. Meschi, R. Moser, M.U. Mozer, M. Mulders, E. Nesvold, M. Nguyen, T. Orimoto, L. Orsini, E. Palencia Cortezon, E. Perez, A. Petrilli, A. Pfeiffer, M. Pierini, M. Pimiä, D. Piparo, G. Polese, L. Quertenmont, A. Racz, W. Reece, J. Rodrigues Antunes, G. Rolandi[30], T. Rommerskirchen, M. Rovere, H. Sakulin, C. Schäfer, C. Schwick, I. Segoni, A. Sharma, P. Siegrist, P. Silva, M. Simon, P. Sphicas[31], M. Spiropulu[3], M. Stoye, P. Tropea, A. Tsirou, P. Vichoudis, M. Voutilainen, W.D. Zeuner

Paul Scherrer Institut, Villigen, Switzerland
W. Bertl, K. Deiters, W. Erdmann, K. Gabathuler, R. Horisberger, Q. Ingram, H.C. Kaestli, S. König, D. Kotlinski, U. Langenegger, F. Meier, D. Renker, T. Rohe, J. Sibille[32]

Institute for Particle Physics, ETH Zurich, Zurich, Switzerland
L. Bäni, P. Bortignon, L. Caminada[33], B. Casal, N. Chanon, Z. Chen, S. Cittolin, G. Dissertori, M. Dittmar, J. Eugster, K. Freudenreich, C. Grab, W. Hintz, P. Lecomte, W. Lustermann, C. Marchica[33], P. Martinez Ruiz del Arbol, P. Milenovic[34], F. Moortgat, C. Nägeli[33], P. Nef, F. Nessi-Tedaldi, L. Pape, F. Pauss, T. Punz, A. Rizzi, F.J. Ronga, M. Rossini, L. Sala, A.K. Sanchez, M.-C. Sawley, A. Starodumov[35], B. Stieger, M. Takahashi, L. Tauscher[†], A. Thea, K. Theofilatos, D. Treille, C. Urscheler, R. Wallny, M. Weber, L. Wehrli, J. Weng

Universität Zürich, Zurich, Switzerland
E. Aguilo, C. Amsler, V. Chiochia, S. De Visscher, C. Favaro, M. Ivova Rikova, B. Millan Mejias, P. Otiougova, P. Robmann, A. Schmidt, H. Snoek

National Central University, Chung-Li, Taiwan
Y.H. Chang, K.H. Chen, C.M. Kuo, S.W. Li, W. Lin, Z.K. Liu, Y.J. Lu, D. Mekterovic, R. Volpe, J.H. Wu, S.S. Yu

National Taiwan University (NTU), Taipei, Taiwan
P. Bartalini, P. Chang, Y.H. Chang, Y.W. Chang, Y. Chao, K.F. Chen, W.-S. Hou, Y. Hsiung, K.Y. Kao, Y.J. Lei, R.-S. Lu, J.G. Shiu, Y.M. Tzeng, X. Wan, M. Wang

Cukurova University, Adana, Turkey
A. Adiguzel, M.N. Bakirci[36], S. Cerci[37], C. Dozen, I. Dumanoglu, E. Eskut, S. Girgis, G. Gokbulut, I. Hos, E.E. Kangal, A. Kayis Topaksu, G. Onengut, K. Ozdemir, S. Ozturk[38], A. Polatoz, K. Sogut[39], D. Sunar Cerci[37], B. Tali[37], H. Topakli[36], D. Uzun, L.N. Vergili, M. Vergili

Physics Department, Middle East Technical University, Ankara, Turkey
I.V. Akin, T. Aliev, B. Bilin, S. Bilmis, M. Deniz, H. Gamsizkan, A.M. Guler, K. Ocalan, A. Ozpineci, M. Serin, R. Sever, U.E. Surat, M. Yalvac, E. Yildirim, M. Zeyrek

Bogazici University, Istanbul, Turkey
M. Deliomeroglu, D. Demir[40], E. Gülmez, B. Isildak, M. Kaya[41], O. Kaya[41], M. Özbek, S. Ozkorucuklu[42], N. Sonmez[43]

Kharkov Institute of Physics and Technology, National Scientific Center, Kharkov, Ukraine
L. Levchuk

University of Bristol, Bristol, United Kingdom
F. Bostock, J.J. Brooke, T.L. Cheng, E. Clement, D. Cussans, R. Frazier, J. Goldstein, M. Grimes, D. Hartley, G.P. Heath, H.F. Heath, L. Kreczko, S. Metson, D.M. Newbold[44], K. Nirunpong, A. Poll, S. Senkin, V.J. Smith

Rutherford Appleton Laboratory, Didcot, United Kingdom
L. Basso[45], K.W. Bell, A. Belyaev[45], C. Brew, R.M. Brown, B. Camanzi, D.J.A. Cockerill, J.A. Coughlan, K. Harder, S. Harper, J. Jackson, B.W. Kennedy, E. Olaiya, D. Petyt, B.C. Radburn-Smith, C.H. Shepherd-Themistocleous, I.R. Tomalin, W.J. Womersley, S.D. Worm

Imperial College, London, United Kingdom
R. Bainbridge, G. Ball, J. Ballin, R. Beuselinck, O. Buchmuller, D. Colling, N. Cripps, M. Cutajar, G. Davies, M. Della Negra, W. Ferguson, J. Fulcher, D. Futyan, A. Gilbert, A. Guneratne Bryer, G. Hall, Z. Hatherell, J. Hays, G. Iles, M. Jarvis, G. Karapostoli, L. Lyons, B.C. MacEvoy, A.-M. Magnan, J. Marrouche, B. Mathias, R. Nandi, J. Nash, A. Nikitenko[35], A. Papageorgiou, M. Pesaresi, K. Petridis, M. Pioppi[46], D.M. Raymond, S. Rogerson, N. Rompotis, A. Rose, M.J. Ryan, C. Seez, P. Sharp, A. Sparrow, A. Tapper, S. Tourneur, M. Vazquez Acosta, T. Virdee, S. Wakefield, N. Wardle, D. Wardrope, T. Whyntie

Brunel University, Uxbridge, United Kingdom
M. Barrett, M. Chadwick, J.E. Cole, P.R. Hobson, A. Khan, P. Kyberd, D. Leslie, W. Martin, I.D. Reid, L. Teodorescu

Baylor University, Waco, USA
K. Hatakeyama, H. Liu

The University of Alabama, Tuscaloosa, USA
C. Henderson

Boston University, Boston, USA
T. Bose, E. Carrera Jarrin, C. Fantasia, A. Heister, J. St. John, P. Lawson, D. Lazic, J. Rohlf, D. Sperka, L. Sulak

Brown University, Providence, USA
A. Avetisyan, S. Bhattacharya, J.P. Chou, D. Cutts, A. Ferapontov, U. Heintz, S. Jabeen, G. Kukartsev, G. Landsberg, M. Luk, M. Narain, D. Nguyen, M. Segala, T. Sinthuprasith, T. Speer, K.V. Tsang

University of California, Davis, Davis, USA
R. Breedon, G. Breto, M. Calderon De La Barca Sanchez, S. Chauhan, M. Chertok, J. Conway, P.T. Cox, J. Dolen, R. Erbacher, E. Friis, W. Ko, A. Kopecky, R. Lander, H. Liu, S. Maruyama, T. Miceli, M. Nikolic, D. Pellett, J. Robles, B. Rutherford, S. Salur, T. Schwarz, M. Searle, J. Smith, M. Squires, M. Tripathi, R. Vasquez Sierra, C. Veelken

University of California, Los Angeles, Los Angeles, USA
V. Andreev, K. Arisaka, D. Cline, R. Cousins, A. Deisher, J. Duris, S. Erhan, C. Farrell, J. Hauser, M. Ignatenko, C. Jarvis, C. Plager, G. Rakness, P. Schlein[†], J. Tucker, V. Valuev

University of California, Riverside, Riverside, USA
J. Babb, A. Chandra, R. Clare, J. Ellison, J.W. Gary, F. Giordano, G. Hanson, G.Y. Jeng, S.C. Kao, F. Liu, H. Liu, O.R. Long, A. Luthra, H. Nguyen, S. Paramesvaran, B.C. Shen[†], R. Stringer, J. Sturdy, S. Sumowidagdo, R. Wilken, S. Wimpenny

University of California, San Diego, La Jolla, USA
W. Andrews, J.G. Branson, G.B. Cerati, D. Evans, F. Golf, A. Holzner, R. Kelley, M. Lebourgeois, J. Letts, B. Mangano, S. Padhi, C. Palmer, G. Petrucciani, H. Pi, M. Pieri, R. Ranieri, M. Sani, V. Sharma, S. Simon, E. Sudano, M. Tadel, Y. Tu, A. Vartak, S. Wasserbaech[47], F. Würthwein, A. Yagil, J. Yoo

University of California, Santa Barbara, Santa Barbara, USA
D. Barge, R. Bellan, C. Campagnari, M. D'Alfonso, T. Danielson, K. Flowers, P. Geffert, J. Incandela, C. Justus, P. Kalavase, S.A. Koay, D. Kovalskyi, V. Krutelyov, S. Lowette, N. Mccoll, V. Pavlunin, F. Rebassoo, J. Ribnik, J. Richman, R. Rossin, D. Stuart, W. To, J.R. Vlimant, C. West

California Institute of Technology, Pasadena, USA
A. Apresyan, A. Bornheim, J. Bunn, Y. Chen, M. Gataullin, Y. Ma, A. Mott, H.B. Newman, C. Rogan, K. Shin, V. Timciuc, P. Traczyk, J. Veverka, R. Wilkinson, Y. Yang, R.Y. Zhu

Carnegie Mellon University, Pittsburgh, USA
B. Akgun, R. Carroll, T. Ferguson, Y. Iiyama, D.W. Jang, S.Y. Jun, Y.F. Liu, M. Paulini, J. Russ, H. Vogel, I. Vorobiev

University of Colorado at Boulder, Boulder, USA
J.P. Cumalat, M.E. Dinardo, B.R. Drell, C.J. Edelmaier, W.T. Ford, A. Gaz, B. Heyburn, E. Luiggi Lopez, U. Nauenberg, J.G. Smith, K. Stenson, K.A. Ulmer, S.R. Wagner, S.L. Zang

Cornell University, Ithaca, USA
L. Agostino, J. Alexander, A. Chatterjee, N. Eggert, L.K. Gibbons, B. Heltsley, K. Henriksson, W. Hopkins, A. Khukhunaishvili, B. Kreis, Y. Liu, G. Nicolas Kaufman, J.R. Patterson, D. Puigh, A. Ryd, M. Saelim, E. Salvati, X. Shi, W. Sun, W.D. Teo, J. Thom, J. Thompson, J. Vaughan, Y. Weng, L. Winstrom, P. Wittich

Fairfield University, Fairfield, USA
A. Biselli, G. Cirino, D. Winn

Fermi National Accelerator Laboratory, Batavia, USA
S. Abdullin, M. Albrow, J. Anderson, G. Apollinari, M. Atac, J.A. Bakken, L.A.T. Bauerdick, A. Beretvas, J. Berryhill, P.C. Bhat, I. Bloch, K. Burkett, J.N. Butler, V. Chetluru, H.W.K. Cheung, F. Chlebana, S. Cihangir, W. Cooper, D.P. Eartly, V.D. Elvira, S. Esen, I. Fisk, J. Freeman, Y. Gao, E. Gottschalk, D. Green, O. Gutsche, J. Hanlon, R.M. Harris, J. Hirschauer, B. Hooberman, H. Jensen, M. Johnson, U. Joshi, B. Klima, K. Kousouris, S. Kunori, S. Kwan, C. Leonidopoulos, P. Limon, D. Lincoln, R. Lipton, J. Lykken, K. Maeshima, J.M. Marraffino, D. Mason, P. McBride, T. Miao, K. Mishra, S. Mrenna, Y. Musienko[48], C. Newman-Holmes, V. O'Dell, J. Pivarski, R. Pordes, O. Prokofyev, E. Sexton-Kennedy, S. Sharma, W.J. Spalding, L. Spiegel, P. Tan, L. Taylor, S. Tkaczyk, L. Uplegger, E.W. Vaandering, R. Vidal, J. Whitmore, W. Wu, F. Yang, F. Yumiceva, J.C. Yun

University of Florida, Gainesville, USA
D. Acosta, P. Avery, D. Bourilkov, M. Chen, S. Das, M. De Gruttola, G.P. Di Giovanni, D. Dobur, A. Drozdetskiy, R.D. Field, M. Fisher, Y. Fu, I.K. Furic, J. Gartner, S. Goldberg, J. Hugon, B. Kim, J. Konigsberg, A. Korytov, A. Kropivnitskaya, T. Kypreos, J.F. Low, K. Matchev, G. Mitselmakher, L. Muniz, C. Prescott, R. Remington, A. Rinkevicius, M. Schmitt, B. Scurlock, P. Sellers, N. Skhirtladze, M. Snowball, D. Wang, J. Yelton, M. Zakaria

Florida International University, Miami, USA
V. Gaultney, L.M. Lebolo, S. Linn, P. Markowitz, G. Martinez, J.L. Rodriguez

Florida State University, Tallahassee, USA
T. Adams, A. Askew, J. Bochenek, J. Chen, B. Diamond, S.V. Gleyzer, J. Haas, S. Hagopian, V. Hagopian, M. Jenkins, K.F. Johnson, H. Prosper, S. Sekmen, V. Veeraraghavan

Florida Institute of Technology, Melbourne, USA
M.M. Baarmand, B. Dorney, S. Guragain, M. Hohlmann, H. Kalakhety, I. Vodopiyanov

University of Illinois at Chicago (UIC), Chicago, USA
M.R. Adams, I.M. Anghel, L. Apanasevich, Y. Bai, V.E. Bazterra, R.R. Betts, J. Callner, R. Cavanaugh, C. Dragoiu, L. Gauthier, C.E. Gerber, D.J. Hofman, S. Khalatyan, G.J. Kunde[49], F. Lacroix, M. Malek, C. O'Brien, C. Silkworth, C. Silvestre, A. Smoron, D. Strom, N. Varelas

The University of Iowa, Iowa City, USA
U. Akgun, E.A. Albayrak, B. Bilki, W. Clarida, F. Duru, C.K. Lae, E. McCliment, J.-P. Merlo, H. Mermerkaya[50], A. Mestvirishvili, A. Moeller, J. Nachtman, C.R. Newsom, E. Norbeck, J. Olson, Y. Onel, F. Ozok, S. Sen, J. Wetzel, T. Yetkin, K. Yi

Johns Hopkins University, Baltimore, USA
B.A. Barnett, B. Blumenfeld, A. Bonato, C. Eskew, D. Fehling, G. Giurgiu, A.V. Gritsan, Z.J. Guo, G. Hu, P. Maksimovic, S. Rappoccio, M. Swartz, N.V. Tran, A. Whitbeck

The University of Kansas, Lawrence, USA
P. Baringer, A. Bean, G. Benelli, O. Grachov, R.P. Kenny Iii, M. Murray, D. Noonan, S. Sanders, J.S. Wood, V. Zhukova

Kansas State University, Manhattan, USA
A.F. Barfuss, T. Bolton, I. Chakaberia, A. Ivanov, S. Khalil, M. Makouski, Y. Maravin, S. Shrestha, I. Svintradze, Z. Wan

Lawrence Livermore National Laboratory, Livermore, USA
J. Gronberg, D. Lange, D. Wright

University of Maryland, College Park, USA
A. Baden, M. Boutemeur, S.C. Eno, D. Ferencek, J.A. Gomez, N.J. Hadley, R.G. Kellogg, M. Kirn, Y. Lu, A.C. Mignerey, K. Rossato, P. Rumerio, F. Santanastasio, A. Skuja, J. Temple, M.B. Tonjes, S.C. Tonwar, E. Twedt

Massachusetts Institute of Technology, Cambridge, USA
B. Alver, G. Bauer, J. Bendavid, W. Busza, E. Butz, I.A. Cali, M. Chan, V. Dutta, P. Everaerts, G. Gomez Ceballos, M. Goncharov, K.A. Hahn, P. Harris, Y. Kim, M. Klute, Y.-J. Lee, W. Li, C. Loizides, P.D. Luckey, T. Ma, S. Nahn, C. Paus, D. Ralph, C. Roland, G. Roland, M. Rudolph, G.S.F. Stephans, F. Stöckli, K. Sumorok, K. Sung, D. Velicanu, E.A. Wenger, R. Wolf, S. Xie, M. Yang, Y. Yilmaz, A.S. Yoon, M. Zanetti

University of Minnesota, Minneapolis, USA
S.I. Cooper, P. Cushman, B. Dahmes, A. De Benedetti, G. Franzoni, A. Gude, J. Haupt, K. Klapoetke, Y. Kubota, J. Mans, N. Pastika, V. Rekovic, R. Rusack, M. Sasseville, A. Singovsky, N. Tambe

University of Mississippi, University, USA
L.M. Cremaldi, R. Godang, R. Kroeger, L. Perera, R. Rahmat, D.A. Sanders, D. Summers

University of Nebraska-Lincoln, Lincoln, USA
K. Bloom, S. Bose, J. Butt, D.R. Claes, A. Dominguez, M. Eads, P. Jindal, J. Keller, T. Kelly, I. Kravchenko, J. Lazo-Flores, H. Malbouisson, S. Malik, G.R. Snow

State University of New York at Buffalo, Buffalo, USA
U. Baur, A. Godshalk, I. Iashvili, S. Jain, A. Kharchilava, A. Kumar, S.P. Shipkowski, K. Smith

Northeastern University, Boston, USA
G. Alverson, E. Barberis, D. Baumgartel, O. Boeriu, M. Chasco, S. Reucroft, J. Swain, D. Trocino, D. Wood, J. Zhang

Northwestern University, Evanston, USA
A. Anastassov, A. Kubik, N. Odell, R.A. Ofierzynski, B. Pollack, A. Pozdnyakov, M. Schmitt, S. Stoynev, M. Velasco, S. Won

University of Notre Dame, Notre Dame, USA
L. Antonelli, D. Berry, A. Brinkerhoff, M. Hildreth, C. Jessop, D.J. Karmgard, J. Kolb, T. Kolberg, K. Lannon, W. Luo, S. Lynch, N. Marinelli, D.M. Morse, T. Pearson, R. Ruchti, J. Slaunwhite, N. Valls, M. Wayne, J. Ziegler

The Ohio State University, Columbus, USA
B. Bylsma, L.S. Durkin, J. Gu, C. Hill, P. Killewald, K. Kotov, T.Y. Ling, M. Rodenburg, C. Vuosalo, G. Williams

Princeton University, Princeton, USA
N. Adam, E. Berry, P. Elmer, D. Gerbaudo, V. Halyo, P. Hebda, A. Hunt, E. Laird, D. Lopes Pegna, D. Marlow, T. Medvedeva, M. Mooney, J. Olsen, P. Piroué, X. Quan, B. Safdi, H. Saka, D. Stickland, C. Tully, J.S. Werner, A. Zuranski

University of Puerto Rico, Mayaguez, USA
J.G. Acosta, X.T. Huang, A. Lopez, H. Mendez, S. Oliveros, J.E. Ramirez Vargas, A. Zatserklyaniy

Purdue University, West Lafayette, USA
E. Alagoz, V.E. Barnes, G. Bolla, L. Borrello, D. Bortoletto, M. De Mattia, A. Everett, A.F. Garfinkel, L. Gutay, Z. Hu, M. Jones, O. Koybasi, M. Kress, A.T. Laasanen, N. Leonardo, C. Liu, V. Maroussov, P. Merkel, D.H. Miller, N. Neumeister, I. Shipsey, D. Silvers, A. Svyatkovskiy, H.D. Yoo, J. Zablocki, Y. Zheng

Purdue University Calumet, Hammond, USA
N. Parashar

Rice University, Houston, USA
A. Adair, C. Boulahouache, K.M. Ecklund, F.J.M. Geurts, B.P. Padley, R. Redjimi, J. Roberts, J. Zabel

University of Rochester, Rochester, USA
B. Betchart, A. Bodek, Y.S. Chung, R. Covarelli, P. de Barbaro, R. Demina, Y. Eshaq, H. Flacher, A. Garcia-Bellido, P. Goldenzweig, Y. Gotra, J. Han, A. Harel, D.C. Miner, D. Orbaker, G. Petrillo, W. Sakumoto, D. Vishnevskiy, M. Zielinski

The Rockefeller University, New York, USA
A. Bhatti, R. Ciesielski, L. Demortier, K. Goulianos, G. Lungu, S. Malik, C. Mesropian

Rutgers, the State University of New Jersey, Piscataway, USA
S. Arora, O. Atramentov, A. Barker, C. Contreras-Campana, E. Contreras-Campana, D. Duggan, Y. Gershtein, R. Gray, E. Halkiadakis, D. Hidas, D. Hits, A. Lath, S. Panwalkar, R. Patel, A. Richards, K. Rose, S. Schnetzer, S. Somalwar, R. Stone, S. Thomas

University of Tennessee, Knoxville, USA
G. Cerizza, M. Hollingsworth, S. Spanier, Z.C. Yang, A. York

Texas A&M University, College Station, USA
R. Eusebi, W. Flanagan, J. Gilmore, A. Gurrola, T. Kamon, V. Khotilovich, R. Montalvo, I. Osipenkov, Y. Pakhotin, A. Safonov, S. Sengupta, I. Suarez, A. Tatarinov, D. Toback, M. Weinberger

Texas Tech University, Lubbock, USA
N. Akchurin, C. Bardak, J. Damgov, P.R. Dudero, C. Jeong, K. Kovitanggoon, S.W. Lee, T. Libeiro, P. Mane, Y. Roh, A. Sill, I. Volobouev, R. Wigmans, E. Yazgan

Vanderbilt University, Nashville, USA
E. Appelt, E. Brownson, D. Engh, C. Florez, W. Gabella, M. Issah, W. Johns, C. Johnston, P. Kurt, C. Maguire, A. Melo, P. Sheldon, B. Snook, S. Tuo, J. Velkovska

University of Virginia, Charlottesville, USA
M.W. Arenton, M. Balazs, S. Boutle, B. Cox, B. Francis, S. Goadhouse, J. Goodell, R. Hirosky, A. Ledovskoy, C. Lin, C. Neu, J. Wood, R. Yohay

Wayne State University, Detroit, USA
S. Gollapinni, R. Harr, P.E. Karchin, C. Kottachchi Kankanamge Don, P. Lamichhane, M. Mattson, C. Milstène, A. Sakharov

University of Wisconsin, Madison, USA
M. Anderson, M. Bachtis, D. Belknap, J.N. Bellinger, D. Carlsmith, S. Dasu, J. Efron, L. Gray, K.S. Grogg, M. Grothe, R. Hall-Wilton, M. Herndon, A. Hervé, P. Klabbers, J. Klukas, A. Lanaro, C. Lazaridis, J. Leonard, R. Loveless, A. Mohapatra, I. Ojalvo, W. Parker, D. Reeder, I. Ross, A. Savin, W.H. Smith, J. Swanson, M. Weinberg

†: Deceased
1: Also at CERN, European Organization for Nuclear Research, Geneva, Switzerland
2: Also at Universidade Federal do ABC, Santo Andre, Brazil
3: Also at California Institute of Technology, Pasadena, USA
4: Also at Laboratoire Leprince-Ringuet, Ecole Polytechnique, IN2P3-CNRS, Palaiseau, France
5: Also at Suez Canal University, Suez, Egypt
6: Also at Cairo University, Cairo, Egypt
7: Also at British University, Cairo, Egypt
8: Also at Fayoum University, El-Fayoum, Egypt
9: Also at Ain Shams University, Cairo, Egypt
10: Also at Soltan Institute for Nuclear Studies, Warsaw, Poland
11: Also at Massachusetts Institute of Technology, Cambridge, USA
12: Also at Université de Haute-Alsace, Mulhouse, France
13: Also at Brandenburg University of Technology, Cottbus, Germany
14: Also at Moscow State University, Moscow, Russia
15: Also at Institute of Nuclear Research ATOMKI, Debrecen, Hungary
16: Also at Eötvös Loránd University, Budapest, Hungary
17: Also at Tata Institute of Fundamental Research—HECR, Mumbai, India
18: Also at University of Visva-Bharati, Santiniketan, India
19: Also at Sharif University of Technology, Tehran, Iran
20: Also at Isfahan University of Technology, Isfahan, Iran
21: Also at Shiraz University, Shiraz, Iran
22: Also at Facoltà Ingegneria Università di Roma, Roma, Italy

23: Also at Università della Basilicata, Potenza, Italy
24: Also at Laboratori Nazionali di Legnaro dell' INFN, Legnaro, Italy
25: Also at Università degli studi di Siena, Siena, Italy
26: Also at Faculty of Physics of University of Belgrade, Belgrade, Serbia
27: Also at University of California, Los Angeles, Los Angeles, USA
28: Also at University of Florida, Gainesville, USA
29: Also at Université de Genève, Geneva, Switzerland
30: Also at Scuola Normale e Sezione dell' INFN, Pisa, Italy
31: Also at University of Athens, Athens, Greece
32: Also at The University of Kansas, Lawrence, USA
33: Also at Paul Scherrer Institut, Villigen, Switzerland
34: Also at University of Belgrade, Faculty of Physics and Vinca Institute of Nuclear Sciences, Belgrade, Serbia
35: Also at Institute for Theoretical and Experimental Physics, Moscow, Russia
36: Also at Gaziosmanpasa University, Tokat, Turkey
37: Also at Adiyaman University, Adiyaman, Turkey
38: Also at The University of Iowa, Iowa City, USA
39: Also at Mersin University, Mersin, Turkey
40: Also at Izmir Institute of Technology, Izmir, Turkey
41: Also at Kafkas University, Kars, Turkey
42: Also at Suleyman Demirel University, Isparta, Turkey
43: Also at Ege University, Izmir, Turkey
44: Also at Rutherford Appleton Laboratory, Didcot, United Kingdom
45: Also at School of Physics and Astronomy, University of Southampton, Southampton, United Kingdom
46: Also at INFN Sezione di Perugia; Università di Perugia, Perugia, Italy
47: Also at Utah Valley University, Orem, USA
48: Also at Institute for Nuclear Research, Moscow, Russia
49: Also at Los Alamos National Laboratory, Los Alamos, USA
50: Also at Erzincan University, Erzincan, Turkey